Characterization of Hydraulic Properties of Potentially Fractured Industrial D Landfill Sites, and A Study of Heterogeneity Effects on Fate and Transport in Groundwater

Work Assignment Manager and Technical Directions:

Dr. Steve Schmelling
U.S. Environmental Protection Agency
National Risk Management Research Laboratory
Subsurface Protection and Remediations Division
Ada, OK 74820

Prepared by:

Dynamac Corporation
3601 Oakridge Blvd.
Ada, OK 74820
Under Contract No. WA3-IR1

U.S. Environmental Protection Agency
National Risk Management Research Laboratory
Subsurface Protection and Remediations Division
Ada, OK 74820

March 1998

Table of Contents

BACKGROUND

The Hazardous Waste Identification Rule (HWIR) is an attempt to reduce the amount of waste that is subject to RCRA Subtitle C regulations. Under this rule, waste that meets certain criteria will exit the Subtitle C regulations and be dealt with under Subtitle D regulations. Wastes that are affected by HWIR are those that are designated as hazardous because they are mixed with, derived from, or contain hazardous wastes. In the proposed rule (Federal Register, Volume 60, #245, pp 66343 - 66469, December 21, 1995), the determination of which wastes will exit the system is based on a modeling risk assessment that evaluates potential exposure pathways from a variety of sources such as waste piles and impoundments. The risk assessment considers both human and ecological risks. The model EPACMTP (EPA, 1996), in conjunction with a Monte Carlo procedure, is used to assess the impact of the rule through the ground-water pathway.

Through an Office of Research and Development (ORD) team, coordinated by the Office of Research and Science Integration (ORSI), the NRMRL/SPRD provided technical review comments to the Office of Solid Waste (OSW) concerning the methodologies utilized for HWIR and the implementation of the proposed rule. This work is in response to OSW's request, through NRMRL/SPRD, for investigating the scientific and technical aspects in the implementation of the Science Plan which was developed by ORD and OSW to address concerns regarding the ground-water pathways of the HWIR.

The specific tasks include: 1) Develop a data base to investigate the extent to which sites that are within the scope of the HWIR are impacted by being located in areas of fractured rock; 2) Investigate the impact of sites located on fractures; 3) Investigate the impact of hydraulic property heterogeneities (*e.g.*, hydraulic conductivity) and the resulting risk analysis.

1. DEVELOPMENT OF FRACTURED ROCK DATA BASE (Task A)

Develop a data base showing the extent to which fractured rock sites are expected to serve as disposal sites for wastes that would exit Subtitle C as a result of HWIR.

Site specific fracture information for each waste management location is vital in determining whether individual waste sites are located over fractured rock formations. However, site specific fracture information over the continental U.S. does not exist and it is impractical to assess the fracture characteristics for each site over the entire nation. Therefore, currently available information such as the regional scale "hydrogeologic environment map" or other available data bases were used to infer the fracture characteristics. Consequently, the available existing data bases were first reviewed to determine which sites are located over or in fractured rock formations, and if ground water is likely to be impacted by the fractures.

Review of Existing Data Bases

The existing data bases include *EPACMTP Background Document* (EPA, 1996) and its background data (OPPI data: EPA, 1986), the Hydrogeologic Database (HGDB) developed by Rice University

for the American Petroleum Institute (API, 1989), and Regional Assessment of Aquifer Vulnerability and Sensitivity of United States (EPA, 1991). A brief review of each existing document or data base is provided below.

EPACMTP: EPA's Composite Model for leachate migration with Transformation Products (EPACMTP) is a simulation model for subsurface fate and transport of contaminants released from land disposal sites. It can predict the ground water exposure in a domestic drinking water receptor well associated with such releases. The composite model consists of a one-dimensional module that simulates infiltration and dissolved constituent transport through the unsaturated zone, which is coupled with a three-dimensional saturated zone module. The saturated zone module consists of three-dimensional ground-water flow and transport sub-modules.

EPACMTP implements a regional, site-based, Monte Carlo approach, as an alternative to the nationwide methodology developed for the Toxicity Characteristic (TC) rule, to derive the nationwide probability distribution of ground water exposure concentration for different types of waste management scenarios. If the national probability distribution of exposure concentrations is known, then the percentage of sites that would be in violation of health standards for a given leachate concentration can be determined. The inference of this percentage forms the basis for the TC and HWIR regulatory efforts.

The model is designed to be used for generic, nationwide assessments using Monte Carlo simulation techniques which require probabilistic input specifications of nationwide hydrogeologic parameters. Note that EPACMTP has limitations on site-specific applications because the model overly simplifies site heterogeneities and fractures. In other words, human and ecological risk assessments, based on the uniform contaminant pathway assumption, become questionable due to the omission of subsurface heterogeneity.

OPPI database: The OPPI survey, conducted in 1986 by Westat Inc. and incorporated in the EPACMTP program, provides the basis for extrapolating the sample inference to the nationwide population. The OPPI data consisted of the four waste management units; landfills, surface impoundments, waste piles and land treatments. Each unit contains site-specific information such as site location (latitude and longitude), area, depth, ground-water temperature, and the corresponding site-climatic region and ground-water region (hydrogeologic environment) for the each individual site. It was found that the individual site location was approximately determined using the postal zip code instead of actual X and Y coordinates. Among the four Waste Management Units presented in EPACMTP (Industrial Subtitle D Landfills, Surface Impoundments, Waste Piles, and Land Application Units), the landfill data was selected in this study for fracture characterization.

HGDB database: The HGDB data was developed by Rice University in 1989. It contains site-specifically surveyed data on ground-water parameters (aquifer thickness, depth to ground water, hydraulic gradient and hydraulic conductivity) for approximately 400 hazardous waste sites throughout the U.S. The HGDB is based on the 111 hydrogeologic settings from the DRASTIC system. DRASTIC ("A Standardized System for Evaluating Ground Water Pollution Potential Using Hydrogeologic Settings," EPA, 1987), in turn, is based on the Heath's (1984) ground-water region and hydrogeologic settings within regions. HGDB condensed the 111 hydrogeologic settings in DRASTIC into 13 hydrogeologic environments (see Table 1.1). The HGDB therefore permits

inferences for regional scale of ground-water parameters on the basis of aquifer type (e.g., metamorphic and igneous, bedded sedimentary rock, sand and gravel, till, etc.). In EPACMTP, the ground-water parameters for a given waste site were assigned by determining the hydrogeologic environment type from the geographic location of the waste site.

Aquifer Vulnerability Report (EPA, 1991): This report, as an independent study from the HGDB, provides a generalized representation of ground-water vulnerability, precipitation distribution, potential well fields, and aquifer sensitivity for each of the 48 conterminous states. To determine aquifer vulnerability, the regional subsurface system was classified according to its physical and hydrogeological characteristics. The classification scheme developed for this report was based on an assessment of the vulnerability of surficial and relatively shallow aquifers to contamination from shallow injection wells and other surface sources. The physical properties that were considered include degree of consolidation, presence of primary porosity and permeability, presence of secondary porosity and permeability (e.g., faults, fractures, joints, solutional features, bedding planes, and others), and presence of intercalated units of different hydraulic characteristics.

The characteristics of individual classes presented in the report are summarized here. In general, aquifers in the 48 conterminous states are classified in four groups; Class I, II, III, and U. Class I is for surficial or shallow permeable units which are highly vulnerable to contamination. Class II is for consolidated bedrock aquifers which are moderately vulnerable. Class III is for consolidated or unconsolidated aquifers that are overlain by more than 50 feet of low permeability material which have low vulnerability. Class U is for undifferentiated aquifers where several lithologic and hydrologic conditions are present within a mappable area.

Class I unit is further divided into four subgroups; Class Ia for unconsolidated aquifers, Class Ib for soluble and fractured bedrock aquifers, Class Ic for semiconsolidated aquifers, and Class Id for covered aquifers (i.e., any Class I aquifers that is overlain by less than 50 feet of low permeability and unconsolidated materials). The Class II unit is also subclassified as higher yield (Class IIa), lower yield (IIb), and covered (IIc) bedrock aquifers.

Table 1.1 Hydrogeologic Environments Classification (from Heath, 1984)

REGION	DESCRIPTION
1	Metamorphic and Igneous
2	Bedded Sedimentary Rock
3	Till Over Sedimentary Rock
4	Sand and Gravel
5	Alluvial Basins Valleys and Fans
6	River Valleys and Floodplains with Overbank Deposit
7	River Valleys and Floodplains without Overbank Deposits

8	Outwash
9	Till and Till Over Outwash
10	Unconsolidated and Semiconsolidated Shallow Aquifers
11	Coastal Beaches
12	Solution Limestone
13	Other (Not classifiable)

Heath, R.C., 1984, State Summaries of Groundwater Resources, U.S. Geological Survey, Water Supply Paper 2275.

Construction of a New Data Base for Fractured Rock Using the Existing Data

To identify the potential fracture occurrence at the existing landfill sites, the fracture characteristics on the regional scale were evaluated utilizing the existing data bases in two different ways; (a) use of the OPPI and HGDB data bases and (b) use of the OPPI data base and the aquifer vulnerability report. It should be noted that the two reports, HGDB and the aquifer vulnerability report, are largely independent of each other. The HGDB provides inferences for regional scale ground-water parameters based on aquifer type (hydrogeologic settings and environments). The aquifer vulnerability report, however, provides a generalized representation of ground-water vulnerability and aquifer sensitivity based on regional scale assessment of physical and hydrogeological characteristics of the subsurface such as degree of soil consolidation, presence of primary and secondary porosity and permeability, precipitation distribution, and location of pumping (receptor) and injection (source of pollution) wells.

The information and maps used in this analysis are regional in nature and provide only a broad, generalized overview of aquifer properties. In other words, the maps were not designed for site-specific evaluations. However, use of the regional scale studies is a practical approach for this project considering the nonexistence of the site specific fracture data, and the objective of the new data base which is the estimation of national screening levels.

Method A. Fracture Assessment Using the OPPI and HGDB Data Bases

The existing OPPI data consisted of the four waste management units: landfills, surface impoundments, waste piles and land treatments. For each given unit, the number of sites belonging to the presumably fractured ground-water regions (e.g., metamorphic and igneous rock, bedded sedimentary rock, till over sedimentary rock, and solution limestone) were divided by the total number of sites to determine the fracture ratio (see the attached Table 1.2). In this process, two methods were employed: non-weighted method and weighted method. For the non-weighted ratio estimation, population density from OPPI was not considered, while the population density was considered for the weighted ratio estimation. The results show that, for the non-weighted estimation, from 45 percent for the landfills (354 over 790 total sites) to 51 percent for the land treatments of existing waste sites are likely to fall into the category of fractured regions. For the weighted estimation, the percentage varied from 44% for the landfill

to 61% for land treatment units. Note that, for the case of weighted ratio, the fracture percentage increased for surface impoundments and land treatments and decreased for landfills and waste piles.

For the landfill units with non-weighted ratios, a total of 354 "fractured" sites were distributed over three hydrogeologic environments: 63 sites on the metamorphic and igneous rock, 137 sites on the bedded sedimentary rock, zero site on the till over sedimentary rock, and 154 sites on the solution limestone. The solution limestone contributed the largest number of fracture sites (154/790 = 19%), while none of the landfill sites belonged to the till over sedimentary rock.

It appears that the estimated fracture ratio is too high and will cause an overestimation of contaminant migration. Keeping in mind that the twelve ground-water regions used in the EPACMTP are based on the regional-scale classification of hydrogeology of the US continent, it is quite possible that many sites belonging to the potentially fractured regions could actually be located in a non-fractured area within the region or the fractures could exist only in the underlying bedrock. In other words, this approach is based on the extremely conservative assumption that if any site belongs to the above four hydrogeologic environments in regional scale it is counted as a "fractured" site. Considering these factors, this preliminary estimation cannot be regarded as representing reality.

Method B. Fracture Assessment Using the OPPI Data and the Aquifer Vulnerability Report

As an alternative, the report "Regional Assessment of Aquifer Vulnerability and Sensitivity in the Conterminous United States, (EPA, 1991)" is used to determine the fracture ratios. The OPPI data for landfills was screened to determine the number of sites belonging to the Soluble and Fractured Bedrock Aquifers (Class Ib) presented in the Aquifer Vulnerability report. The screening was conducted by superimposing the landfill data (latitude and longitude of each site) onto the aquifer vulnerability map of each State from the EPA report.

From a total of 784 landfill sites found in the OPPI data base, 126 sites (about 16 percent) were marked as belonging to Class Ib (see Table 1.3). However, one half (63) of the 126 sites were located on the borderline between Class Ib and other classes in the state maps. In this study those sites were conservatively included in Class Ib. Further, note that an additional 19 out of the 126 Class Ib sites were underlain by lower permeability materials (variably-covered aquifers). Considering these factors, the actual number of sites belonging to the Class Ib is likely to be lower than 126.

Table 1.2 Fracture Ratio from OPPI and HGDB Data Bases

(No. of Sites Located Presumably at the Fractured Hydrogeologic Environment vs Total No. of Sites)

Out of 13 Hydrogeologic Environments (Table 2.2 of EPACMTP Background Document), Hydraulic Environment Numbers 1, 2, 3, and 12 are considered having fractures.

A) Non-Weighted Ratio (Population Density was Not Considered)

Waste Management	Total # of	HE 1		HE 2		HE 3		HE 12		Total Fractured Sites	
Unit	Sites	# of Sites	Ratio (%)	# of Sites	Ratio (%)	# of Sites	Ratio (%)	# of Sites	Ratio (%)	# of Sites	Ratio (%)
Landfills	790	63	8%	137	17%	0	0%	154	19%	354	45%
Surface											
Impoundments	1777	222	12%	287	16%	0	0%	303	17%	812	46%
Waste Piles	827	71	9%	148	18%	0	0%	168	20%	387	47%
Land Treatments	311	53	17%	46	15%	0	0%	61	20%	160	51%

B) Weighted Ratio (Population Density was Considered)

Waste Management	Total # of	HE 1		HE 2		HE 3		HE 12		Total Fractured Sites	
Unit	Sites	# of Sites	Ratio (%)	# of Sites	Ratio (%)	# of Sites	Ratio (%)	# of Sites	Ratio (%)	# of Sites	Ratio (%)
Landfills	2132	184	9%	291	14%	0	0%	465	22%	940	44%
Surface											
Impoundments	5847	907	16%	1148	20%	0	0%	811	14%	2866	49%
Waste Piles	4106	311	8%	713	17%	0	0%	763	19%	1787	44%
Land Treatments	1806	344	19%	454	25%	0	0%	303	17%	1101	61%

Note: HE 1 stands for Hydrogeologic Environment 1 (= Metamorphic &
HE 2 stands for Hydrogeologic Environment 2 (= Beded
HE 3 stands for Hydrogeologic Environment 3 (= Till Over
HE 12 stands for Hydrogeologic Environment 12 (= Solution

Table 1.3 Classification of 784 landfill sites according to the aquifer vulnerability classes

Total # of Sites	Vulnerability Class			
	Ib	Ibv	Ib*	Sum
784	43	19	63	126
%	5.5 %	2.4%	8.0%	16%

An explanation of the vulnerability classifications in Table 1.3 is based on the Aquifer Vulnerability Report and these classifications are briefly summarized below.

Class Ib (Soluble and Fractured Bedrock Aquifers) --- Under the Class I Aquifer (surficial or shallow, permeable units; highly vulnerable to contamination) classification, "lithologies the Class Ib include limestone, dolomite, and, locally, evaporitic units that contain documented karst features or solution channels, regardless of size. ... Also included in this class are sedimentary strata, and metamorphic and igneous rocks that are significantly faulted, fractured, or jointed. In all cases ground-water movement is largely controlled by secondary openings. Well yield ranges are variable, but the important feature is the potential for rapid vertical and lateral ground-water movement along preferred pathways, which results in a high degree of vulnerability (EPA, 1991, pages 6-7)."

Subclass v (Variably-covered Aquifers) --- The modifier "v," such as Class Ibv, is used to describe areas where an undetermined or highly variable thickness of low permeability sediments overlie the major water bearing zone. The "v" indicates that a variable thickness of low permeability material covers the aquifer, to a large degree, and controls vulnerability (Page 8 of the same report).

Additional Mark "*" (Borderline in the Regional Scale Map) --- The latitude and longitude of each site were superimposed on the state's aquifer vulnerability map to determine whether the site is located in the fractured zone or non-fractured zone. In doing so, for many sites, it was not clear from the regional scale map, whether to declare them as fractured or non-fractured. These sites were marked as "Ib*."

The detail information of Table 1.3 for each landfill site is presented in Appendix A, which contains the name of the facility, its latitude and longitude, vulnerability class, and other descriptive data.

Discussion and Comparison of the Two Results

As shown in the Tables 1.2 and 1.3, the estimated ratio of the number of fractured sites over the total number of sites based on the vulnerability report (16%) is much less than the estimation (45%) which was based on the HGDB data base. The main reason for this discrepancy is that, in

OPPI and HGDB analysis, four groups of hydrogeologic environments were considered; while in the OPPI and Vulnerability analysis, only the soluble and fractured bedrock were considered. Note that the ratio of 16% based on the vulnerability report (Table 1.3) becomes comparable with the HGDB based fracture ratio of 19% when only the solution limestone is considered (HE 12 in Table 1.2).

Because each landfill site location was approximately determined using the postal zip code, there is a possibility that some of the Class Ib* sites (located at the borderline) may not actually belong to the Class Ib classification if the exact coordinate systems for each site were to be used. Then, the estimated ratio of number of fractured site over total sites (16 % from Table 1.3) would be further lowered. Considering these uncertainties, the estimated fractured site ratio should only be considered as a qualitative assessment. No one should attempt to use this fracture ratio at the site-specific level characterization. Even for national level evaluation, the estimated fracture ratio needs more field data to reduce the uncertainty.

2. IMPACT OF FRACTURE SYSTEMS ON RISK ANALYSIS PROTOCOL (Task B)

Evaluate the impact of the fractured rock sites in the OSW data bases on the risk analysis for the ground-water pathway.

Under the Hazardous Waste Identification Rule (HWIR), risk-based constituent-specific exit levels for low-risk solid waste are one of the essential elements used to determine whether wastes will exit the Subtitle C regulations and be dealt with under Subtitle D regulations. The risk-based exit levels are established using the risk assessment protocol. Currently, the EPACMTP model is being used in the risk assessment protocol to evaluate the potential exposure pathway and the specific-constituent exit levels. A Monte Carlo approach for the nationwide assessment was used in EPACMTP as one of the essential elements in the risk analysis protocol.

Variation of Hydraulic Conductivity (Review of HGDB Database)

In the EPACMTP, the hydrogeologic parameters (aquifer thickness, depth to groundwater, hydraulic gradient and hydraulic conductivity) are obtained from the survey results of approximately 400 hazardous waste sites. This is known as the HDGB database (API, 1989). The HGDB database, developed by Rice University for API, consists of twelve hydrogeologic environments based on the USGS classification of aquifer regions (Heath, 1984). It provides the summary statistics of the hydrogeologic parameters; the shape and range of the field data distributions (e.g., box plots and histograms). The statistical summary for the hydraulic conductivity shows the national average mean, median and standard deviation of the hydraulic conductivity as 0.647, 0.005, and 0.2184 cm/sec, respectively (see Tables 2.1 and 2.2, and Figure 2.1). The non-sand & gravel hydrogeologic environments showed lower hydraulic conductivities than the sand & gravel environments.

Note that, contrary to the hydrogeologic intuition, the solution limestone environment showed lower hydraulic conductivities than the sand & gravel environments. This could mean that the number of sites belonging to the solution limestone environment (only 11 sites out of 379 total sites) is not large enough to represent a statistically unbiased property. For the solution limestone, a low standard deviation (ranked second lowest among the twelve in Table 2.1) and the smallest range of conductivity value spreading (Figure 2.1) also indicate the potential skew of the selected samples and statistically small sample size.

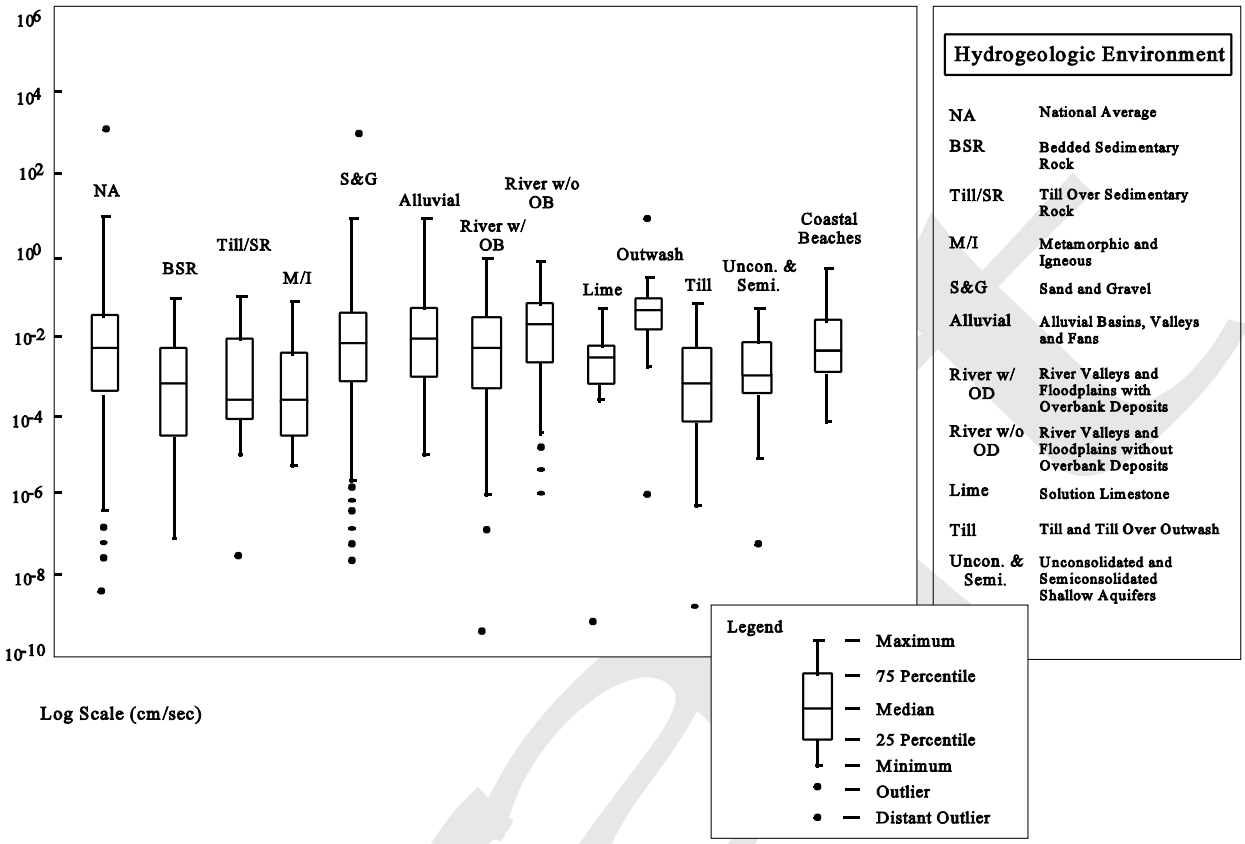

Figure 2.1 Statistics of Hydraulic Conductivity for each Hydrogeologic Environment (from API, 1989)

Table 2.1 Surveyed Hydraulic Conductivity (cm/s) for 12 Hydrogeologic Environments (From the HGDB database: API, 1989)

Hydrogeologic Environment	Number of Class	Median	Geometric *Mean	Arithmetic Mean	Standard deviation
National Average	287	0.0050	0.0026	0.6470	0.2184
Metamorphic/Igneous	19	0.00025	0.0003	0.0910	0.3800
Bedded Sedimentary Rocks	51	0.00028	0.0004	0.0120	0.0270
Till Over Sedimentary Rocks	13	0.0005	0.0003	0.0110	0.0220
Sand & Gravel	191	0.0080	0.0026	0.0915	0.2640
River Valleys With Overbank	20	0.0060	0.0018	0.0920	0.2126
River Valleys Without Overbank	26	0.0200	0.0076	0.1106	0.2300
Alluvial Basins, Valleys & Fans	36	0.0070	0.0058	0.0804	0.1755
Outwash	22	0.0470	0.0328	0.1630	0.4320
Till & Till Over Outwash	20	0.0009	0.0004	0.0067	0.0158
Unconsolidated & Semiconsolidated	18	0.0010	0.0012	0.1078	0.4403
Coastal Beaches	18	0.0065	0.0059	0.0954	0.2486
Solution Limestone	11	0.0040	0.0020	0.0084	0.1390

Median = median of untransformed data
* Mean = the geometric mean is a more representative measure of a lognormal distribution
Hydraulic conductivity reported in cm/second

Table 2.2 Log hydraulic conductivity and standard deviation of Log K (From the HGDB database: API, 1989)

Hydrogeologic Environment	Mean	Standard deviation
National Average	-2.6290	1.6060
Metamorphic/Igneous	-3.417	1.279
Bedded Sedimentary Rocks	-3.395	1.591
Till Over Sedimentry Rocks	-3.421	1.833
Sand & Gravel	-2.414	1.605
River Valleys With Overbank	-2.659	2.171

River Valleys Without Overbank	-2.159	1.668
Alluvial Basins, Valleys & Fans	-2.187	1.429
Outwash	-1.511	1.175
Till & Till Over Outwash	-3.441	1.478
Unconsolidated & Semiconsolidated	-2.865	1.369
Coastal Beaches	-2.050	1.025
Solution Limestone	-2.811	1.175

Mean - mean of transformed data
Hydraulic conductivity reported in cm/second

It can also be postulated that the individual waste sites, although they belong to the solution limestone in regional scale classification, were located in a soil medium which does not have crevices such as fracture-like or karst-like voids in local scale. In addition, considering the fact that more than half of the hydraulic conductivity analyses were performed using the slug test (51.7%, see Table 2.3) and the slug test usually represents only a small area outside the well screen, it is likely that the aquifer test may have missed a large fractured zone in the solution limestone environment.

Table 2.3 Hydraulic Conductivity Measurements (From the HGDB database: API, 1989)

Method	number of responses	percentage of 379 responses
Pump test (& others)	184	48.5 %
Slug test (& others)	196	51.7 %
Lab analysis (& others)	63	16.6 %
Grain size analysis (& others)	72	19.9 %
Literature / Engineering judgement (alone)	144	30.1 %

Note: at some locations, multiple tests (analyses) were performed

Hydraulic Conductivity Increase for Fractured Sites

To evaluate the impact of fractured systems, the hydraulic conductivity of sites which were classified as "potentially fractured" in Section 1(Task A) needs to be increased. Based on factors such as the degree of fracture, interconnectedness, and orientation, past research indicated that

the hydraulic conductivity for fractured media can be greater by several orders of magnitude than the values for the primary porous media. Table 2.4 shows the summary of a recent literature survey.

Table 2.4 Estimation of the multiplier based on the reported hydraulic conductivity in fractured and unfractured subsurface media.

Aquifer Formation	Fractured (K_f)	Unfractured (K_u)	Estimated multiplier	Sources
Clay-rich till	(0.9 - 2100) x 10^{-10} m/s	2 x 10^{-10} m/s	0.5 - 1,050	(1)
Claystone	6.8 x 10^{-7} m/s (1-10) x10^{-8} m/s	1.5 x 10^{-8} m/s (0.1 - 10) x 10^{-10} m/s	45 10 - 10,000	(2)
Clayey till	(4-8400) x 10^{-10} m/s	4.5 x 10^{-10} m/s	1-2,000	(3)
Used in discrete fracture models			100 - 1,000,000	(4)
Permeability	1x 10^{-12} cm^2	2x 10^{-15} cm^2	500	(5)
Unsaturated Zone	9.2 x 10^{-5} m/s 8.2 x 10^{-5} m/s	3.6 x 10^{-6} m/s 1.2 x 10^{-6} m/s	26 68	(6)
Shale, siltstone, sandstone	(0.035 - 1.3)x10^{-2} m/s	(0.035 - 0.17)x10^{-2} m/s	0.2 - 37	(7)
Fracture zone at Finnsjon, Sweden	0.017 - 0.97 m/s	1.0 x 10^{-3} m/s	17 - 970	(8)
Crystalline rock	(0.1 - 3.0) x 10^{-7} m/s	(0.1 - 1.0) x 10^{-9} m/s	10 - 3,000	(9)
Schist, granite, & pegmatite	(0.1 - 1.0) x 10^{-4} m^2/s	(0.1 - 1.0) x 10^{-8} m^2/s	1,000 - 100,000	(10)
Tuff, Yucca Mountain	(1 - 10) x 10^{-6} m/s	3 x 10^{-7} m/s	3.33 - 33.3	(11)
Plutonic rock	1 x 10^{-13} m^2	(0.01 - 1.0) x 10^{-15} m^2	100 - 10,000	(12)

Sources

(1) McKay, L.D., J.A. Cherry, and R.W. Gillham, 1993. Field Experiments in a Fractured Clay Till Hydraulic Conductivity and Fracture Aperture. Water Resources Research 29(4):1149-1162.

(2) Thackston, J., Y. Meeks, J. Stranberg, and H. Tuchfeld, 1989. Characterization of a Fracture Flow Groundwater System at a Waste Management Facility. Proc. of the Third National Outdoor Action Conference on Aquifer Restoration, Ground Water Monitoring and Geophysical Methods. May 22-25, 1989, National Water Well Association, pp.1079-1091.

(3) Fredericia, J., 1990. Saturated Hydraulic Conductivity of Clayey Tills and the Role of Fractures. Nordic Hydrology, 21:119-132.

(4) Odling, N.E., and I. Webman, 1991. A "Conductance" Mesh Approach to the Permeability of Natural and Simulated Fracture Patterns. Water Resources Research 27(10):2633-2643.
(5) Kischinhevsky, M. and P.J. Paes-Leme, 1997. Modeling and Numerical Simulations of Contaminant Transport in Naturally Fractured Porous Media. Transport in Porous Media, 26:25-49.
(6) Ray, C., T.R. Ellsworth, A.J. Valocchi, and C.W. Boast, 1997. An improved dual porosity model for chemical transport in macroporous soils. Journal of Hydrology, 193:270-292.
(7) Gburek, W.J. and J.B. Urban, 1990. The Shallow Weathered Fracture Layer in the Near-Stream Zone. Ground Water 28(6):875-883.
(8) Gustafsson, E. and P. Anderson, 1991. Groundwater flow conditions in a low-angle fracture zone at Finnsjon, Sweden. Journal of Hydrology 126:79-111.
(9) Shapiro, A.M., 1993. The Influence of Heterogeneity in Estimates of Regional Hydraulic Properties in Fractured Crystalline Rock. Memoires of the XXIVth Congress of IAH, AS, Oslo, pp 125-136.
(10) Hsieh, P.A. and M. Shapiro, 1996. Hydraulic Characteristics of Fractured Bedrock Underlying the FSE Well Field at the Mirror Lake Site, Grafton County, New Hampshire. U.S. Geological Survey, Water-Resources Investigations Report 94-4015, 1:127-128.
(11) Bredehoeft, John D., 1997. Fault Permeability near Yucca Mountain. Water Resources Research 33(11), pp.2459-2463.
(12) Ophori, D.U, T. Chan, and F.W. Stanchell, 1998. Hydrologic Response to Pumping and Contaminant Advection in a Fractured Rock Environment. J. of the American Water Resources Association 34(1), pp. 57-72.

Table 2.4 demonstrates that the hydraulic conductivity of fracture media increases by a factor of ten to thousands compared to non-fractured media. The above cited references (except the papers (4) and (11)) show actual field and laboratory measurements of hydraulic conductivity values both for the fractured and non-fractured (primary soil matrix) media. The 4th paper (Odling and Webman, 1991) simulated a discrete fracture flow model with increased conductivity from a hundred to a million times compared to the conductivity value of the primary soil matrix. The 11th paper (Bredehoeft, 1997) estimated the permeability of a fault zone using an equivalent porous medium model by comparing the simulated results against the observed earth-tide water-level fluctuations at a proposed nuclear repository. In the last article (Ophori et al., 1998), slug and pumping tests were conducted to determine the porous media equivalent hydraulic conductivity of 1 x 10^{-13} m^2 at major interconnected fractures. For the back ground rock matrix, which has varying degree of fractures, the permeability values of 1 x 10^{-15} and 1 x 10^{-17} m^2 were used in a finite element simulation.

Using the reported ranges of K_f and K_u values, the multiplier values shown in Table 2.4 were determined such that they varied over the widest possible range. In the 1st paper of McKay et al. (1993), for example, the lower end multiplier of 0.5 was estimated by dividing the lower end of K_f (0.9x10^{-10} m/s) by K_u (2x10^{-10} m/s). Similarly, the upper end multiplier of 1,050 was estimated by dividing the upper end value of K_f by K_u (2,100 x 10^{-10} / 2 x 10^{-10} = 1,050). For the article of Thackston et al. (1990), an extreme case of possible multiplier range was considered. Specifically, the lower end of the K_f values was divided by the upper end of K_u to estimate the minimum multiplier range (1x10^{-8}/10x10^{-10} = 10), while the upper end of K_f was divided by the lower end of K_u to get the maximum multiplier (10x10^{-8}/0.1x10^{-10} = 10,000). The rest of the multiplier values were determined in a similar manner.

Assigning the Hydraulic Conductivity Multiplier in the EPACMTP Simulation

The porous media models require the equivalent hydraulic conductivity for the fracture network instead of the discrete fracture permeability. The equivalent continuum approach is based on the assumption that the study area is large enough and contains highly interconnected fractures. Therefore, the groundwater flux and solute transport are considered as not being significantly influenced by any individual fracture or its interconnections with other fractures (NRC, 1996). In Table 2.4, generally speaking, smaller values of the multiplier were determined from the equivalent conductivity approach while higher values were determined from the discrete fracture permeability measurements. For example, the smaller multiplier values of 45 (Thackston et al, 1989) and 3.33 - 33.3 (Bredehoeft, 1997) were estimated by the equivalent continuum models. The recent paper (Ophori et al., 1998) shows higher ratios (from 100 to 10,000) for these models.

Since the two selected codes (EPACMTP and MODFLOW-SURFACT) are designed for simulation of the porous media approach instead of the discrete fracture, lower end multiplier values from Table 2.4 appear to better represent the fracture conductivity. Therefore, a range of multipliers was selected (5 - 1,000) such that it conservatively covers the table values of multipliers based on the equivalent continuum models (Table 2.5). To account for the uncertainty in fracture identification in the previous section, a lesser value of multiplier was assigned for fractures at the sites marked with either "Ibv" or "Ib*." When compared to the sites marked "Ib," the fractures at the sites marked with Ibv and Ib* were considered to be less permeable due to the sediment overlie (Ibv) and the questionable fracture characterization of the location (Ib*) in the vicinity of borderline, respectively. Therefore, for the sites classified with Ibv and Ib*, the proposed multiplier values were lowered by half to represent smaller permeability. The following table contains the suggested hydraulic conductivity multipliers for different aquifer vulnerability classifications.

Table 2.5 Suggested hydraulic conductivity multipliers for the fractured sites

Class Ib			Class Ibv or Ib*		
Min	Geometric Mean	Max	Min	Geometric Mean	Max
10	100	1,000	5	50	500

The source code of EPACMTP needed to be modified to incorporate the conductivity multiplier in the process of Monte Carlo simulation. Based on the project management's recommendation, the source code modification and execution were performed by the code developer, HydroGeoLogic, Inc., located at Herndon, Virginia.

Preliminary Assessment

As a preliminary trial, the following values (Table 2.6) were suggested initially to give HydroGeoLogic Inc. a framework to start modifying the EPACMTP source code.

Table 2.6 Preliminary trial values of hydraulic conductivity multipliers for the sites classified as belonging to the potentially fractured zones

Class Ib			Class Ibv or Ib*		
Min	Geometric Mean	Max	Min	Geometric Mean	Max
1	10	100	1	5**	50

** This value of 5 was calculated by taking the geometric mean of halves of Min and Max in Class Ib (i.e., 1/2=0.5 and 100/2=50). But the unchanged value of Min (1) was used in Class Ibv or Ib*.

Methodology

In the Monte Carlo simulation, the process is the same as shown in the EPACMTP manual (EPA, 1996) except for the increase of hydraulic conductivity for the fractured sites. The original distribution patterns of hydrogeologic input parameters were used following the methods described in the manual. For the sites marked as "fractured" in the previous section, however, the hydraulic conductivity, determined via the conventional method in EPACMTP, was raised by using a randomly selected multiplier from the Table 2.6. In this process, a triangular distribution was used as a weighting function so that a value near the median can be selected more often than the extremes.

The log-transformed values of the multipliers are assumed to be in the triangular distribution. For the case of Class Ib in the above table, using the triangular distribution density function, 75% of randomly generated multiplier values would range from $10^{0.5} = 3.16$ to $10^{1.5} = 31.6$. Note that the power 0.5 is the logarithmic average of minimum and median values ({log(1) + log(10)}/2), and 1.5 is the logarithmic average of median and maximum ({log(10) + log(100)}/2). Therefore, in the preliminary assessment, the hydraulic conductivity for the fractured media was increased by an average factor of 10 compared to the porous media conductivity.

If the number of simulations is sufficiently large in the Monte Carlo approach, it can be assumed that approximately 16 percent (the ratio of fractured sites versus total number of sites) of total number of simulations were affected by the conductivity change. The increased hydraulic conductivity will cause the pollutant to travel faster. The results from the two simulation cases, one for fractured media and the other for non-fractured media, were compared to evaluate the

fracture impact on the contaminant transport in the porous media. Due to time constraints, only the preliminary trial values were simulated by HydroGeoLogic, Inc. and the results are discussed below.

Results and Discussion

Using the multiplier specified in Table 2.6, 10,000 Monte Carlo simulations (EPACMTP) were performed by HydroGeoLogic, Inc. and the results were compared to the scenario with the no-fracture scenario. Figure 2.2 illustrates the change in hydraulic conductivity distribution caused by the increase of hydraulic conductivity in the fractured sites. The conductivity distribution for the fractured sites is shifted toward the right compared to non-fractured sites. Figures 2.3 and 2.4 show the simulation results of two scenarios: non-fractured and fractured media. The two figures show the normalized concentration versus concentration percentiles. Based on the preliminary multiplier range assumed in Table 2.6, the impact of fractures appears minimal; there is negligible difference in the percentiles.

It was found that this minimal impact of fractured media was partially attributed to the way the receptor well location was determined in Monte Carlo simulation in EPACMTP. For each Monte Carlo simulation, the hypothetical receptor well location was randomly selected based on the nationwide distribution of well location (see Table 2.7). Therefore, each simulated receptor well concentration in Monte Carlo approach varied according to the randomly selected well location. For example, according to the cumulative probability of distance to nearest receptor well for landfill (Table 2.7), less than 10 % of wells are located at 103.6 meter (340 feet) or nearer from the landfill. This probability decreased to 5 percent at 45.7 meter (150 feet). Apparently the impact of hydraulic conductivity variation will be diminished at a well located farther away from the landfill. Moreover, the y- and z-distances from the plume centerline to the receptor well will further reduce the effect of hydraulic conductivity variation under the steady-state uniform flow condition.

If the receptor well location is fixed at one location along the plume centerline, the impact of hydraulic conductivity increase for fracture will become more prominent. The other factors such as random selection of waste site and the hydrogeologic parameters for the selected site will also influence the impact of fracture. Lastly, although it was not included in this report, when the range of multiplier suggested in Table 2.5 (10 to 1,000) is used, the change in normalized concentration due to fractures will become greater. In the next phase of the study, it is suggested that these aspects be investigated in detail.

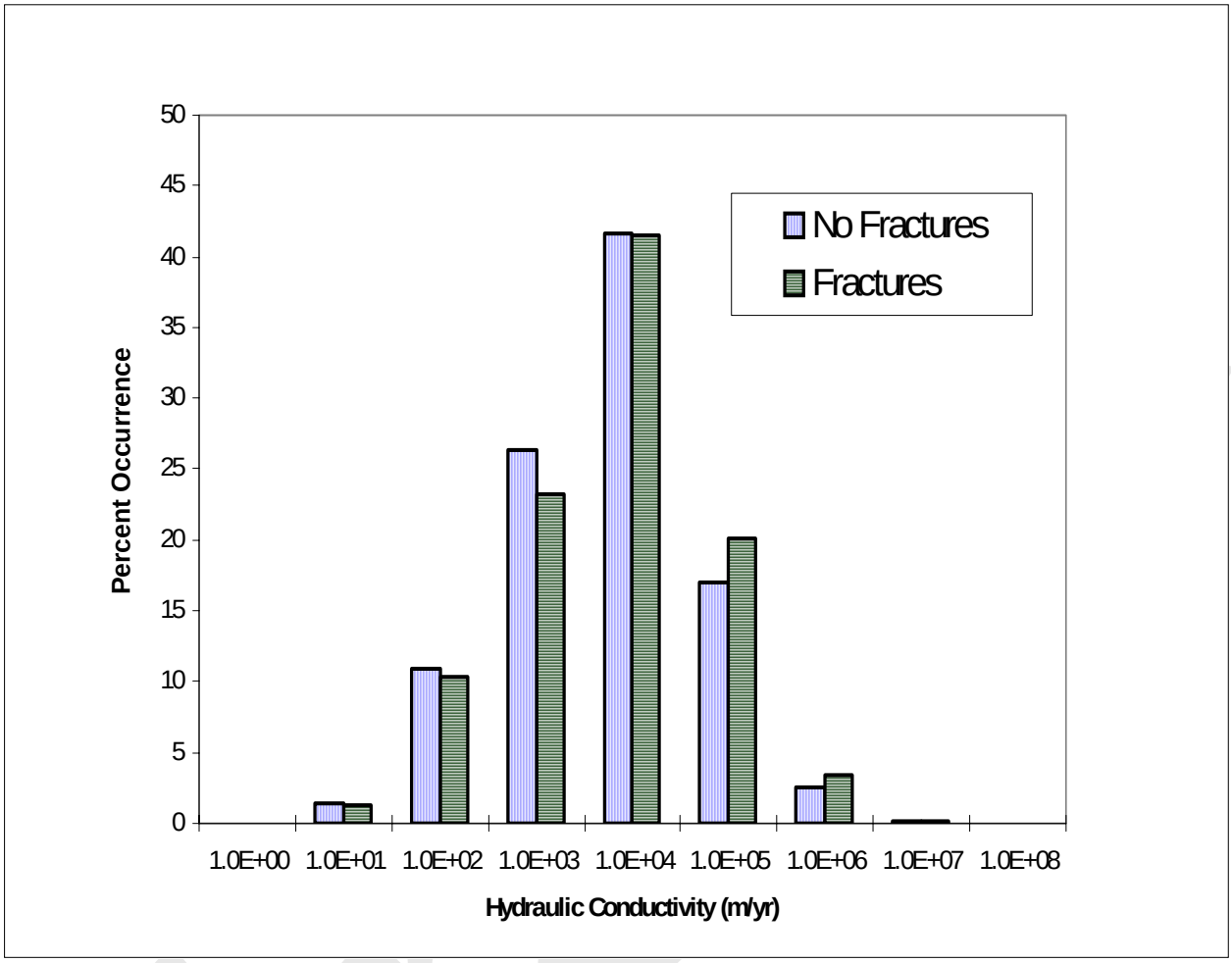

Figure 2.2 Effect of Fracture Analysis on Hydraulic Conductivity Distribution

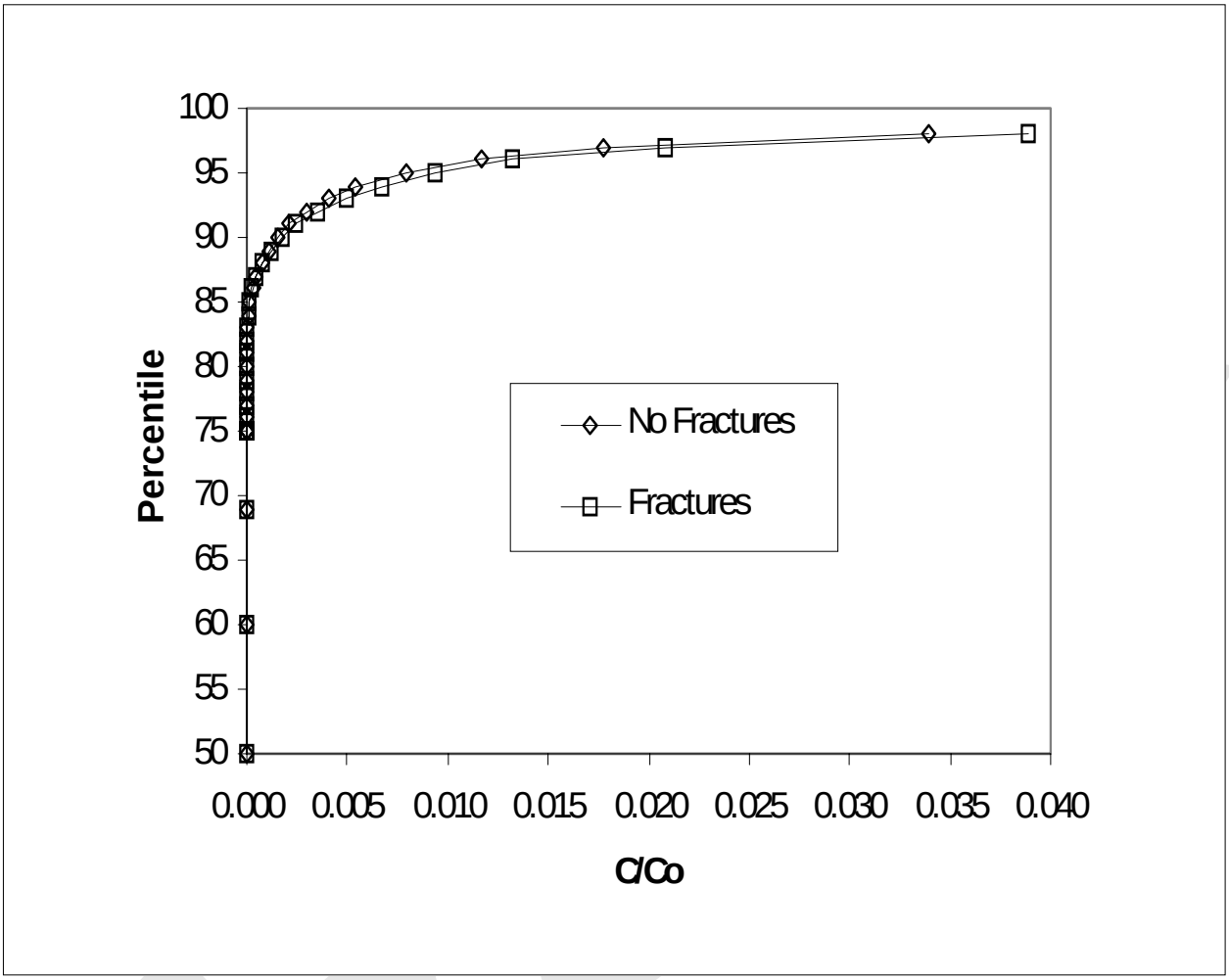

Figure 2.3 Impact of Hydraulic Conductivity Increase on Receptor Well Concentration

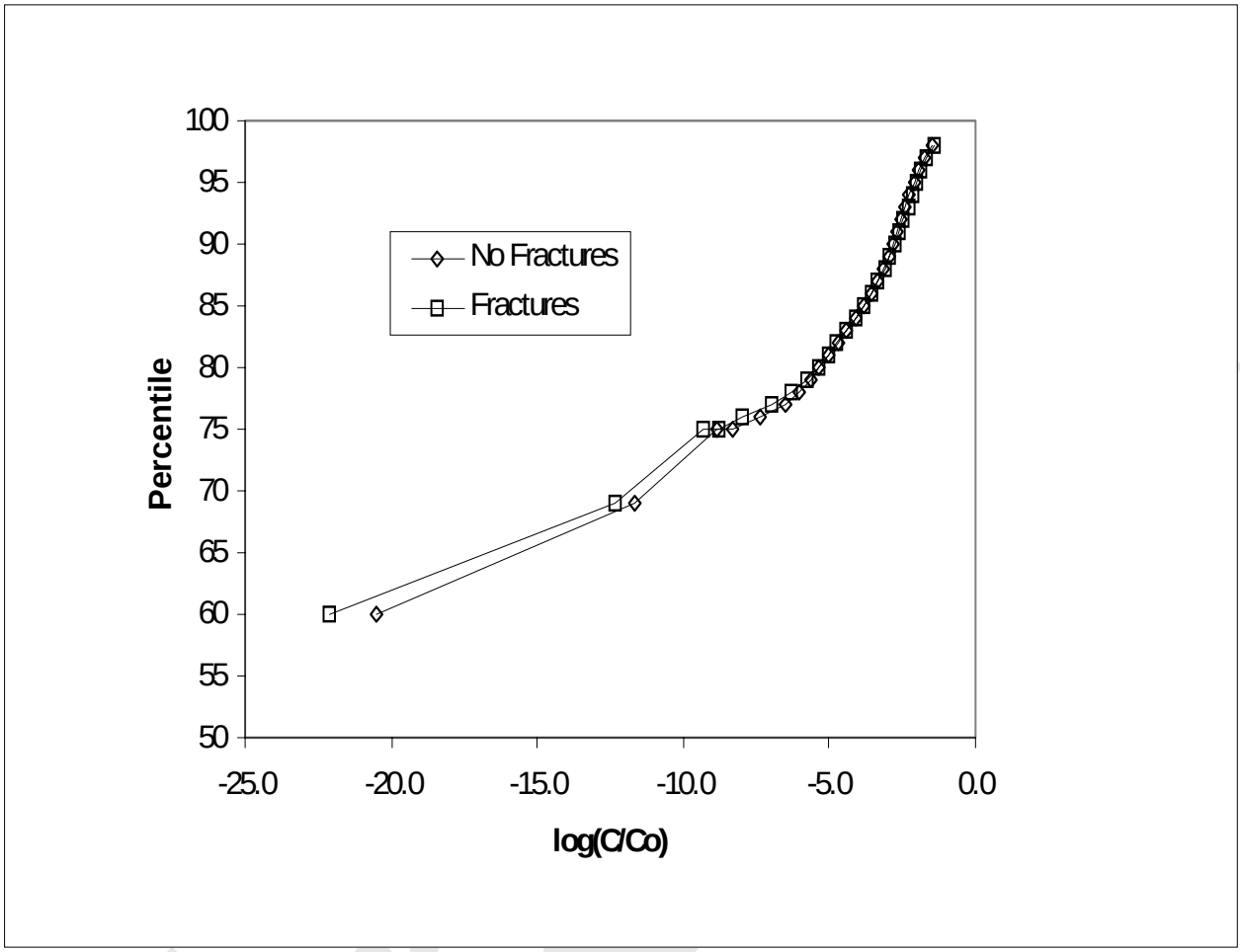

Figure 2.4 Impact of Hydraulic Conductivity Increase on Receptor Well Log Concentration

Table 2.7. Cumulative probability of distance to nearest receptor well for landfills (*from EPA CMTP User's Manual (EPA, 1997*))

Cumulative Probability	***Distance (R) (m)***
0.0	0.6
0.03	13.7
0.04	19.8
0.05	45.7
0.10	103.6
0.15	152.4
0.20	182.9
0.25	243.8
0.30	304.8
0.35	304.8
0.40	365.7
0.45	396.2
0.50	426.7
0.55	457.2
0.60	609.6
0.65	762.0
0.70	804.6
0.75	868.6
0.80	914.4
0.85	1158.2
0.90	1219.1
0.95	1371.5
0.98	1523.9
1.00	1609.3

3. IMPACT OF HETEROGENEOUS HYDRAULIC PROPERTIES ON RISK ANALYSIS PROTOCOL (Task C)

Investigate the impact of neglecting variability in hydraulic conductivity for porous media as a result of the layering of different geologic materials on the outcome of the HWIR analysis.

In the proposed Hazardous Waste Identification Rule (HWIR, Federal Register, Volume 60, pp 66344-66469, December, 1995), the development of the rule for the waste is based on a risk assessment using the EPACMTP model. Since the presence of heterogeneity of hydraulic conductivities is not considered in the EPACMTP, the impact of heterogeneity on HWIR is not known. Therefore, the objective of this study is to examine the impact of heterogeneity on the resulting risk analysis using EPACMTP.

Numerous investigations have been devoted to the impact of heterogeneity of hydraulic conductivities on flow and solute transport in porous media (Dagan, 1982; Dagan, 1984; Schafer and Kinzelbach, 1992; Quinodoz and Valocchi, 1993; Goodrich and McCord, 1995). In general, the presence of heterogeneities in hydraulic properties enhances the dispersion of a dissolved contaminant as it travels over large distances, increasing the contaminant spread (Sudicky, 1986). In a bioremediation study, Schafer and Kinzelbach (1992) found that the heterogeneity of hydraulic conductivity led to a decrease in the overall pollutant removal rate compared to the homogeneous case. Kaluarachchi (1996) observed a rapid reduction of free oil recovery rate in the heterogeneous media. In an analysis of the transport of sorbing solute in aquifers with heterogeneous hydraulic conductivity, Valocchi (1989) and Quinodoz and Valocchi (1993) demonstrated that the overall longitudinal spatial variance of the aqueous-phase solute plume could be expressed as the sum of the variance due to conductivity heterogeneity and that due to adsorption kinetics.

Methodology

To evaluate the impact of heterogeneity (especially hydraulic cunductivities) of the medium, a hypothetical solute transport model was constructed to compare the simulation results for two cases: one using the homogeneous hydraulic conductivity value and the other for heterogeneous values. EPACMTP was used for the homogeneous case while the selected code was used for the heterogeneous case.

<u>Selection of Computer Code for Heterogeneous Medium Case</u>

To choose an appropriate code for heterogeneous aquifer simulation, scores of publically available groundwater model were evaluated for their attributes. Among the listed models in Table 3.1, three codes (MODFLOWT, MODFLOW-SURFACT, and MODMOC-3D) were the first choices. The other codes also have some strong points as well as weak points. However, these three codes are considered relatively superior for the HWIR project due to their usability, CPU time, and public acceptance. In addition, only the saturated zone codes were considered

Table 3.1 Attributes of the potential codes for assessing the impact of heterogeneity of hydraulic properties on the risk analysis protocol.

Code Name	Type		Satura-tion		Flow Con-dition		Medium			Dimensiona- lity			Type of Boundary Conditions						Transport Processes					Usability	
													Flow			Transport									
	Flow	Transport	Saturated	Unsaturated	Steady	Transient	Homogeneous	Heterogeneous	Fracture	One	Two	Three	1st	2nd	3rd	1st	2nd	3rd	Advection	Dispersion	Adsorption	Degradation	Metal	User Interfaces	Documentation
AQUA	x	x	x			x	x	x		x	x	x	x	x	x	x	x		x	x	x	x		yes	good
2DFEMFAT	x	x	x	x		x	x	x		x	x		x	x	x	x	x		x	x	x	x		no	--
FRACMAN	x	x				x			x	x	x		x	x		x			x	x	x			yes	avg
FTWORK	x	x	x			x	x	x		x	x	x	x	x	x	x	x		x	x	x	x		no	--
HYDROGEO CHEM	x	x	x	x		x	x	x		x	x		x	x	x	x	x	x	x	x	x		x	no	good
HYDRUS-2D (SWMS-2D)	x	x	x	x		x	x	x		x	x		x	x	x	x	x	x	x	x	x	x		yes	good
MODFLOWT	x	x	x			x	x	x		x	x	x	x	x	x	x	x		x	x	x	x		yes	--
MODFLOW-SURFACT	x	x	x			x	x	x		x	x	x	x	x	x	x	x		x	x	x	x		yes	good
MODMOC-3D	x	x	x			x	x	x		x	x	x	x	x	x	x	x		x	x	x	x		--	--
PORFLOW	x	x	x			x	x	x	x	x	x		x	x	x	x	x	x	x	x	x			yes	good
SUTRA	x	x	x	x		x	x	x		x	x		x	x	x	x	x		x	x	x	x		yes	good
SWIFT	x	x	x			x	x	x	x	x	x	x	x	x	x	x	x		x	x	x	x		yes	--
TARGET	x	x	x	x		x	x	x		x	x		x	x	x	x	x		x	x	x			yes	good
VS2DT	x	x	x	x		x	x	x		x	x		x	x	x	x	x		x	x	x	x		yes	good

since there is no vadose zone to simulate in the hypothetical model. For all the three codes, MODFLOW was used as a flow module. For the transport module, FTWORK is used in MODFLOWT, and MOC is used in MODMOC-3D. In the MODFLOW-SURFACT, a new module was developed for transport simulation. All three existing programs (MODFLOW, FTWORK, and MOC) have been widely used for many years in the subsurface modeling community. Based on the code developers' claim on the computational efficiency of each code, MODFLOW-SURFACT was finally selected.

Hypothetical Test Problem

A numerical conceptual model was developed to assess the impact of aquifer heterogeneity on the contaminant transport. The steady-state saturated aquifer system of uniform thickness was assumed. This hypothetical aquifer system was based on the second verification problem shown in the background document of EPACMTP (EPA, 1996). A rectangular model was considered as shown in Figure 3.1 with 20 meter wide by 20 meter long square landfill source located atop of aquifer of 30 meter thickness. In horizontal plane, the aquifer is 500 meter long and 220 meter wide. There is 0.1 m/y of water recharge through the landfill source and zero elsewhere. The recharge water was assumed to have a contaminant concentration of 100 mg/L. A specified head boundary condition was imposed at the left and right sides (x = 0 and 500 meters) so that the ambient groundwater is unidirectional and its gradient was 0.015 m/m. The contaminant was subject to slight degradation ($\lambda = 0.01\ y^{-1}$) and moderate retardation (R=3.0). Table 3.2 shows the flow and transport parameters. The aquifer hydraulic conductivity is 630 m/y (= 0.0020 cm/s), which represents the geometric mean of solution limestone hydrogeologic environments. As shown in Table 2.1, the selected value of 0.0020 cm/s is close to the national average (0.0026) and smaller than the conductivity of sand and gravel (0.0026) and alluvial basins (0.0058).

Table 3.2 Flow and Transport Parameters for an Example Problem

Parameter	Value
Infiltration rate, I	0.1 m/y
Recharge rate outside of landfill, I_r	0.0 m/y
Hydraulic conductivity, k_x	630 m/y
Longitudinal dispersivity (horizontal), α_L	5.0 m
Transverse dispersivity (horizontal), α_T	1.0 m
Vertical dispersivity, α_V	0.5 m
Molecular diffusion coefficient, D_d^*	0.0 m^2/sec
Porosity, φ	0.25
Degradation coefficient, λ	0.01 y^{-1}

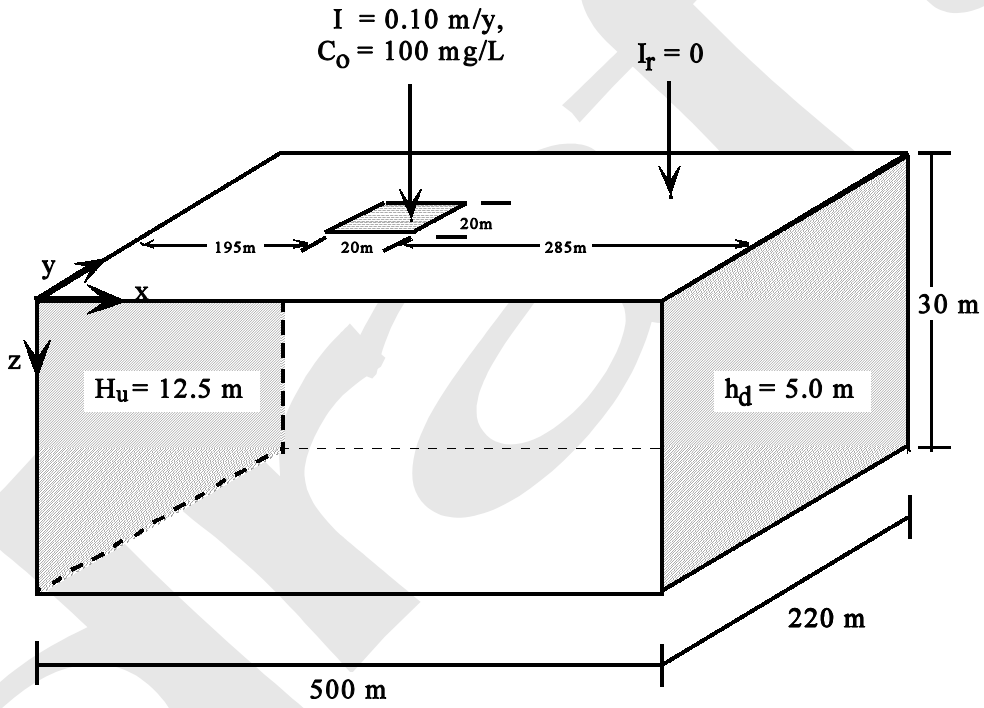

Figure 3.1 A three-dimensional conceptual model with variable recharge.

Generation of Heterogeneous Hydraulic Conductivity

A computer code called TUBA (Zimmerman and Wilson, 1990), which was based on the turning bands algorithm (Delhomme, 1976; Mantoglou and Wilson, 1982; Tompson et al., 1989), was used to generate vertical two-dimensional random realizations of the heterogeneous hydraulic conductivity. The hydraulic conductivity was assumed to be log-normally distributed with mean (log(630) = 2.8) and variance (0.4). Note that the assumed variance of 0.4, which is equivalent to the standard deviation of 0.632, is considerably smaller than the standard deviations of Log K in Table 2.2. To be consistent with the small scale of the hypothetical landfill test case, a smaller varince than the one in national scale was used.

Figure 3.2 depicts the heterogeneity and anisotropy of the hydraulic conductivity for a selected realization which was generated by TUBA. Although the conductivity contours in vertical cross section may vary for each TUBA realization, the general pattern of anisotropy (horizontal stratification) was maintained throughout all the realizations by providing the control parameters of X and Y directional correlation lengths (100:10). In TUBA, the higher ratio of correlation in X and Y directions results in more anisotropy, and vise versa.

Variation of generated hydraulic conductivity depends on the input parameter values for TUBA (e.g., variance and spatial correlation). Based on the 1,000 realizations performed, the simulated mean hydraulic conductivity varied two orders of magnitude when the variance of 0.2 was used and the degree of variation went up to 5 orders of magnitude with the input variance of 0.4. Figure 3.3 shows the hydraulic conductivity variation when the TUBA input variance of 0.4 was used. For each realization, the geometric mean was calculated by taking antilogarithm of the arithmetic mean of the logarithms of the conductivity values at each node in the vertical cross section. Then an ensemble average of the geometric means was calculated by the taking the arithmetic average of the geometric means over the number of realizations. As shown in Figure 3.3, the ensemble average becomes invariable as the number of realizations increases (after 400 realizations it became almost constant). Therefore, to save the computational CPU time, the number of Monte Carlo simulations was limited to 500.

Modeling Setup

Solute transport was evaluated for 50 years of simulation time. In the beginning, 5 years of pollutant leaching (100 mg/L) from the landfill was assumed. After leaching for 5 years into the aquifer system, the source was assumed to be removed. An observation point was selected at 55 meters downgradient from the edge of landfill along the plume centerline at the top row (x = 270, y = 110, z = 0 meters). The aquifer was treated as homogeneous in transverse horizontal direction (y-coordinate direction). For a higher resolution, the numerical grid in x-direction was refined to 5 m at the landfill source which is one half of the regular grid size (10 meters) for outside of landfill. In the y-coordinate direction, Δy was set as 10 meters for the non-source area while the 20 meter long landfill source was divided into five irregular grids (6, 3, 2, 3 and 6 meters). In the vertical direction, 6 layers were used (5 meters of uniform thickness for each layer).

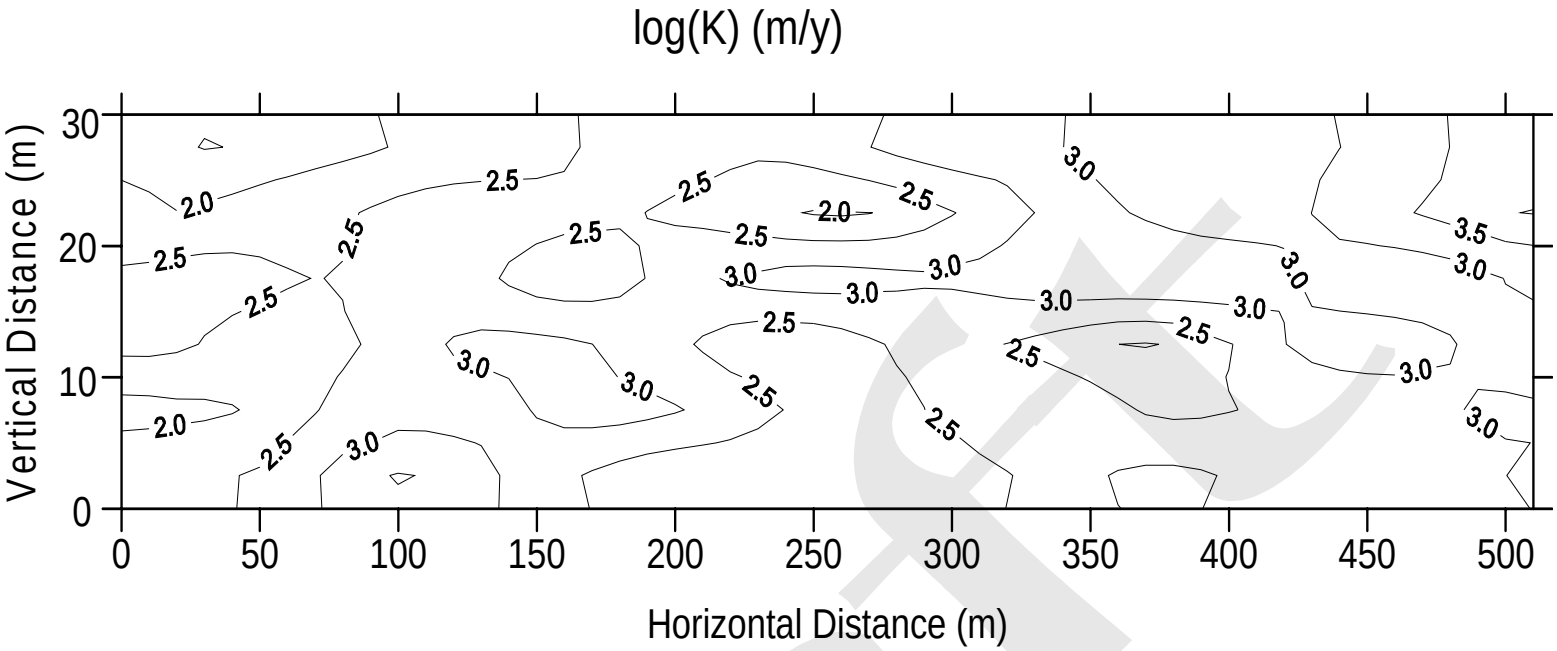

Figure 3.2 TUBA generated hydraulic conductivity distribution contour (from a single realization).

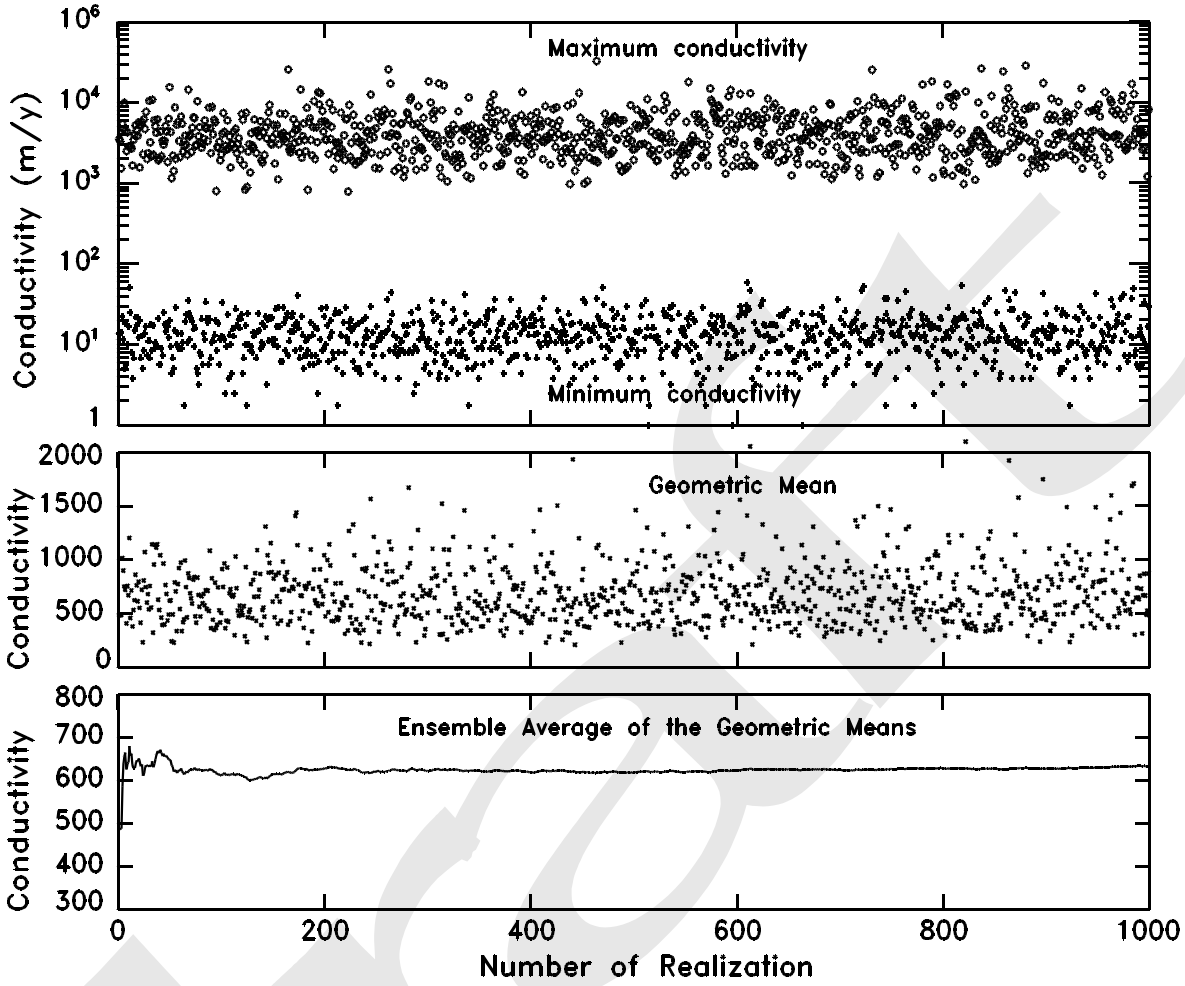

Figure 3.3. Variation of TUBA generated hydraulic conductivity values and geometric means.

Simulation Scenarios

Several simulation scenarios were set up to evaluate the aquifer heterogeneity impact (see Table 3.3). First, the hypothetical problem was analyzed by single run simulations using the two codes (EPACMTP and MODFLOW-SURFACT). The purpose of this scenario was to compare the simulation results from the two computer codes. The two codes were run twice each; two times for EPACMTP (one with analytical solution option, and the other with the numerical solution), and two times for MODFLOW-SURFACT (one with homogeneous conductivity, and the other with heterogeneous conductivity).

According to the EPACMTP manual, use of the analytical solution is restricted to situations where the vertical influx of water (infiltration and recharge) is negligibly small compared to the horizontal groundwater flow in the system (e.g., it was recommended that the ratio should be less than 0.02). To select the numerical solution option in EPACMTP, a small value of maximum flux ratio (QRMAX = 0.0001, see the users manual) was used to specify the flow ratio (vertical versus horizontal). Also, it was found by trial and error that the number of observation points (n_{obs}) times the observation times (n_t) in the input file should be smaller than 21 to use the built-in analytical solution in EPACMTP (i.e., $n_{obs} \times n_t \leq 20$).

Next, Monte Carlo simulations were performed using the hydraulic conductivities generated by TUBA. For the EPACMTP simulation (with numerical solution option), the geometric mean of the heterogeneous conductivity was used for each run. For the MODFLOW-SURFACT, the TUBA generated heterogeneous hydraulic conductivities were used for all 500 executions.

Table 3.3 Simulation Scenarios

	Single run		Monte Carlo (500 runs)	
Computer Code	Homogeneous	Heterogeneous	Homogeneous	Heterogeneous
EPACMTP (Analytical)	✓			
EPACMTP (Numerical)	✓		✓	
MODFLOW-SURFACT (Numerical)	✓	✓	✓	✓

Note: ✓ means the scenario was simulated.

Results and Discussion

Single Simulation

According to the simulation scenario, the homogeneous problem was solved three times using

the two codes. As shown in Figure 3.4, the results were similar although the peak concentrations varied in the three approaches. The two concentration curves from EPACMTP simulation showed lower peaks than that of MODFLOW-SURFACT. For the numerical solution of EPACMTP, the 3-dimensional aquifer space was automatically discretized by a processing utility included in the program. The program code does not allow the user to change or determine the grid size. Moreover, neither the user's manual nor the simulation output reveals how the discretization was done. Therefore, it only can be postulated that the differences in simulation results may have been due to the different discretization methods (at least partially).

The single run of the heterogeneous problem showed a much lower peak concentration (SURFACT, heterogeneous case in Figure 3.4). Also, as expected, it was shown that the pollutant moved faster than in the homogeneous case. The lower peak concentration and quicker arrival time were attributed to the enhanced contaminant dispersion and potential preferential pathways caused by the soil heterogeneity.

Monte Carlo Simulation

As stated in the previous section, a Monte Carlo method was used by running the selected model with 500 different hydraulic conductivities for each run. For the homogeneous scenario, the geometric mean of the TUBA generated hydraulic conductivity values were used for each simulation. For the heterogeneous case, the TUBA generated heterogeneous conductivity values were directly used for each simulation. Figures 3.5 and 3.6 depict the results of MODFLOW-SURFACT simulations (500 runs) for the homogeneous and heterogeneous cases, respectively. For the homogeneous case, simulated peak concentrations ranged approximately from 0.4 to 1.0 mg/L, and the corresponding time for the peak concentrations was ranged from 5 to 15 years approximately. For the heterogeneous case, the extent of variation was larger; the peak concentrations varied from 0.2 to 1.05 mg/L approximately, and the peak arrival times were from 3 to greater than 50 years. Although it is not shown in this report, the Monte Carlo simulation of EPACMTP for the homogeneous scenario resulted in a pattern similar to the homogeneous MODFLOW-SURFACT simulations.

A statistical inference from the Monte Carlo simulation was attempted by estimating the probability distribution function (PDF) of concentrations at a given time. A selected percentile from the PDF reveals the likelihood of multiple simulation results falling into a certain range of concentration. For example, for the EPACMTP homogeneous simulation results in the Figure 3.7 (dotted lines), there is 90 percent probability (from 0.05 to 0.95 percentiles) that the simulated concentration at 10 years will be greater than approximately 0.1 mg/L and less than 0.8 mg/L. In other words, out of 500 total simulations, 450 simulations (90 percent) resulted in the concentration range of 0.1 to 0.8 mg/L at 10 years after the landfill began leaching. At t=20 years, there is 5 percent probability that the concentration will be 0.22 mg/L or higher. Or, it also can be interpreted that there is 95 percent probability that the concentration will be 0.22 mg/L or less at 20 years. Similar results were obtained from the homogeneous MODFLOW-SURFACT simulation except for the higher peak concentration (see the dotted line in Figure 3.8).

Several other phenomena were observed when the results were compared between homogeneous

and heterogeneous cases (Figures 3.7 and 3.8). For the homogeneous case, the concentrations at later times were smaller than the corresponding concentrations for the heterogeneous case. Incidentally, the magnitude of peak concentration was higher in the homogeneous case compared

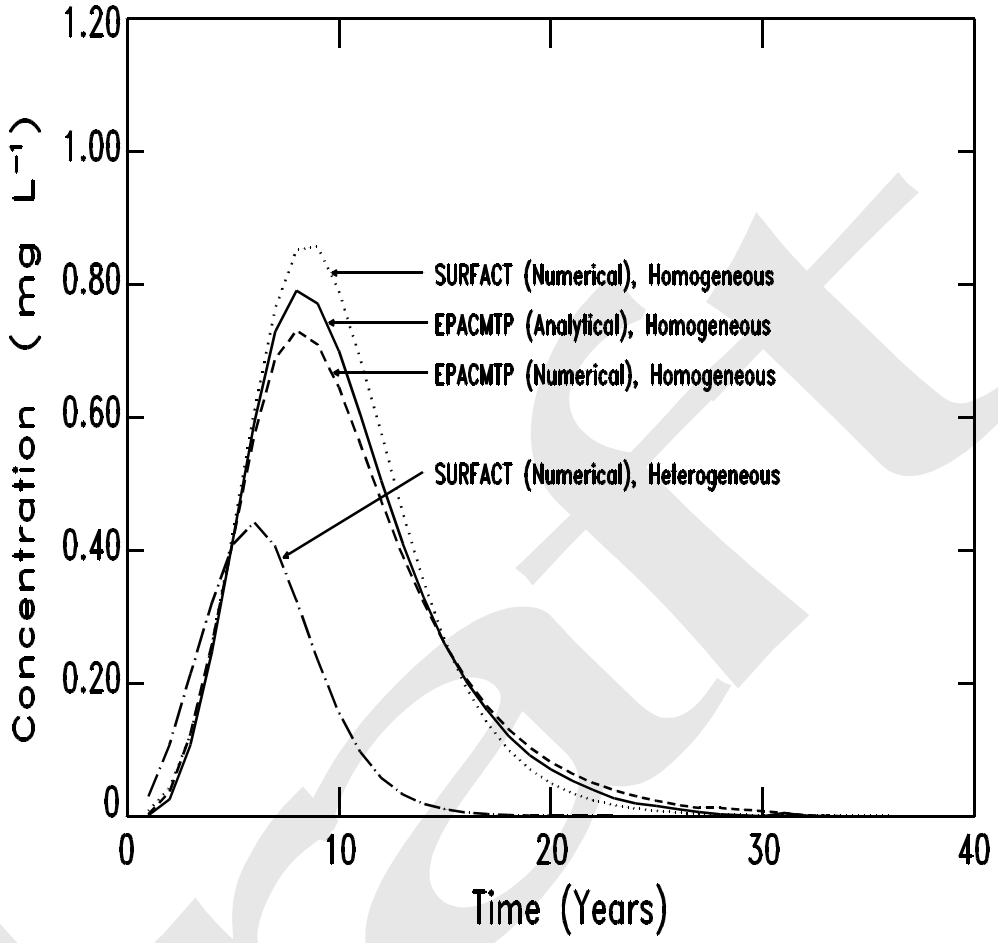

Figure 3.4. Comparison of the single run results at the observation point (55 meters downgradient from the edge of source). A hydraulic conductivity of 465 m/y is used.

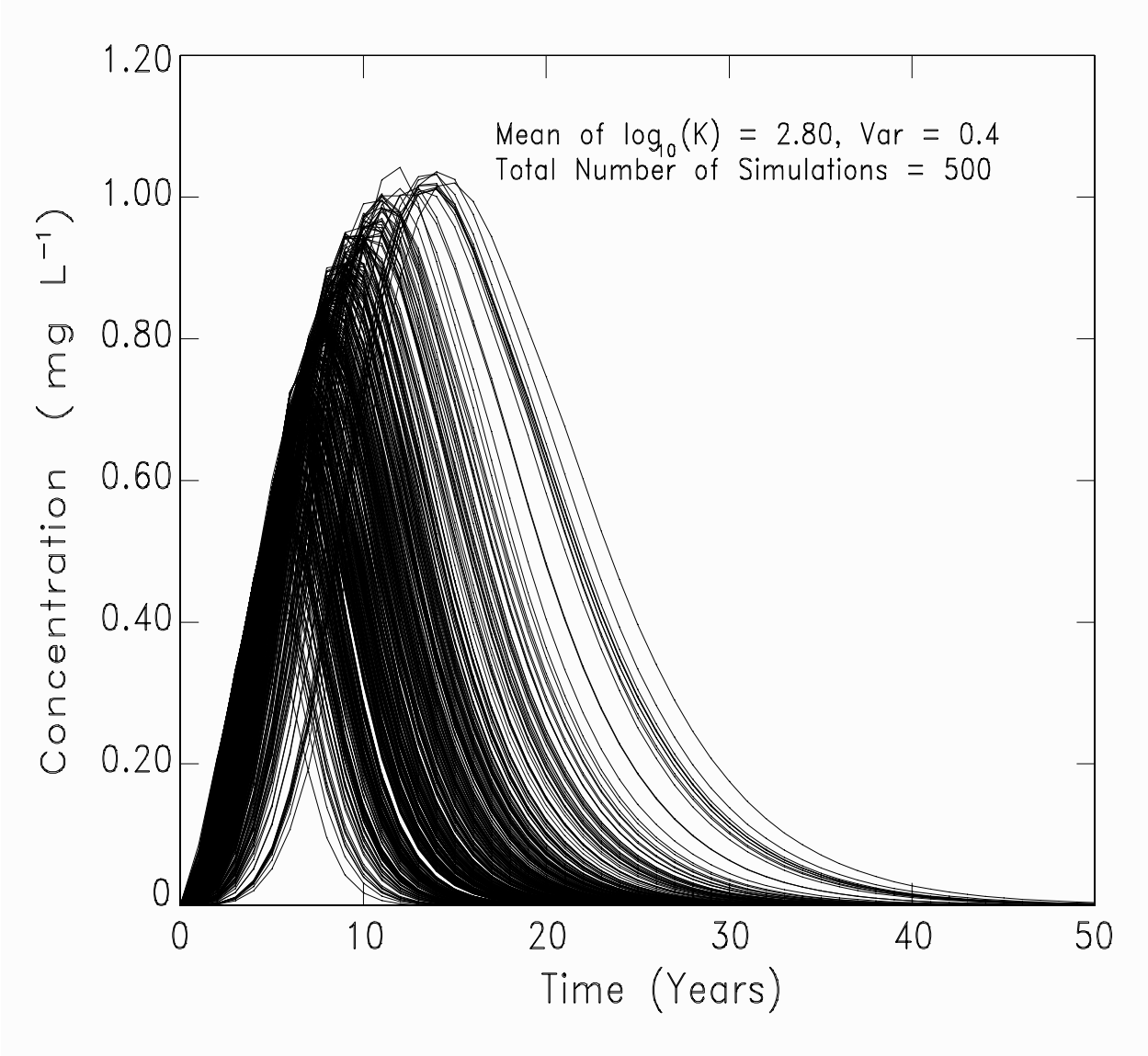

Figure 3.5. Results of MODFLOW-SURFACT simulations with homogeneous hydraulic conductivity.

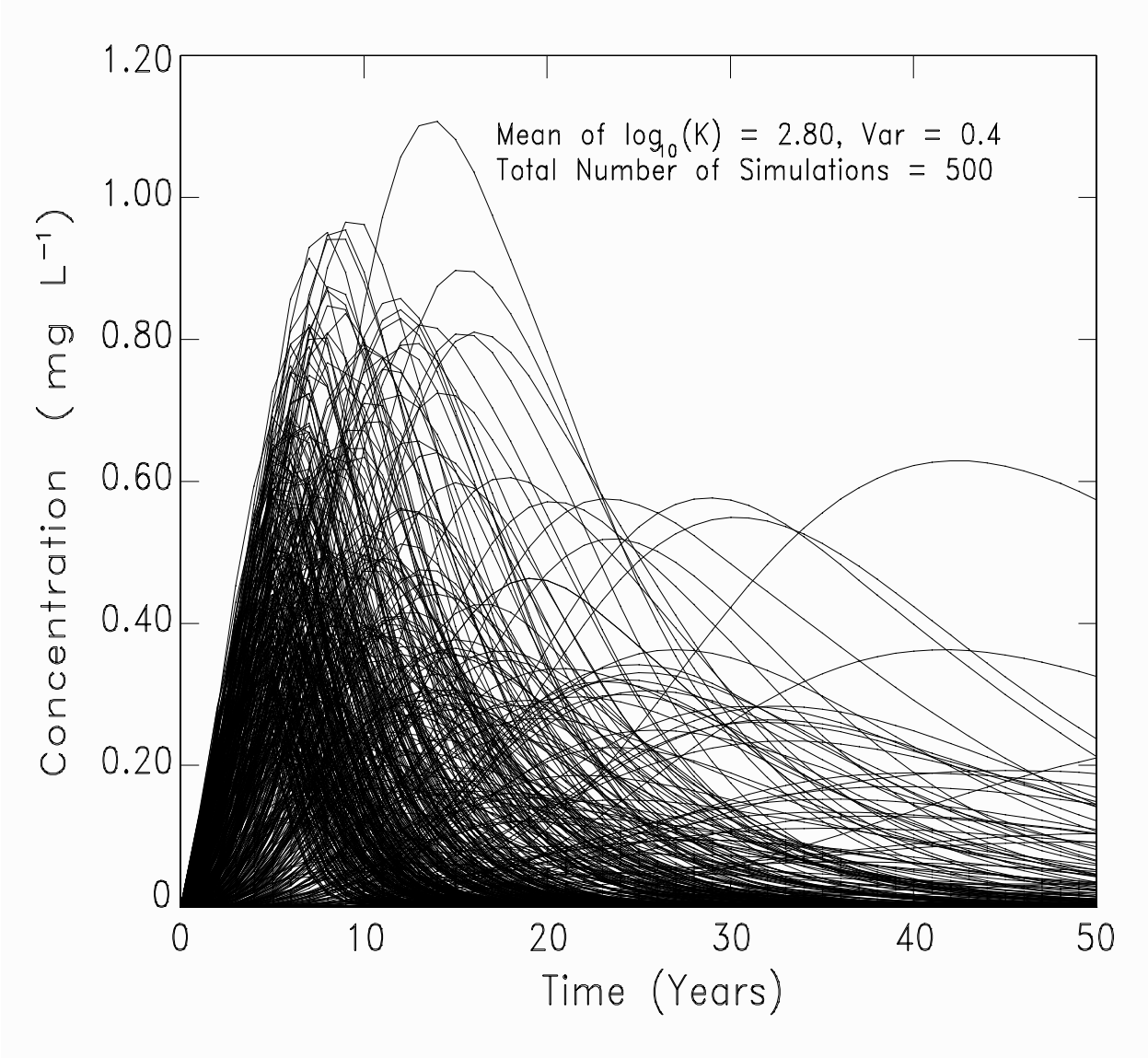

Figure 3.6. Results of MODFLOW-SURFACT simulations with heterogeneous hydraulic conductivity.

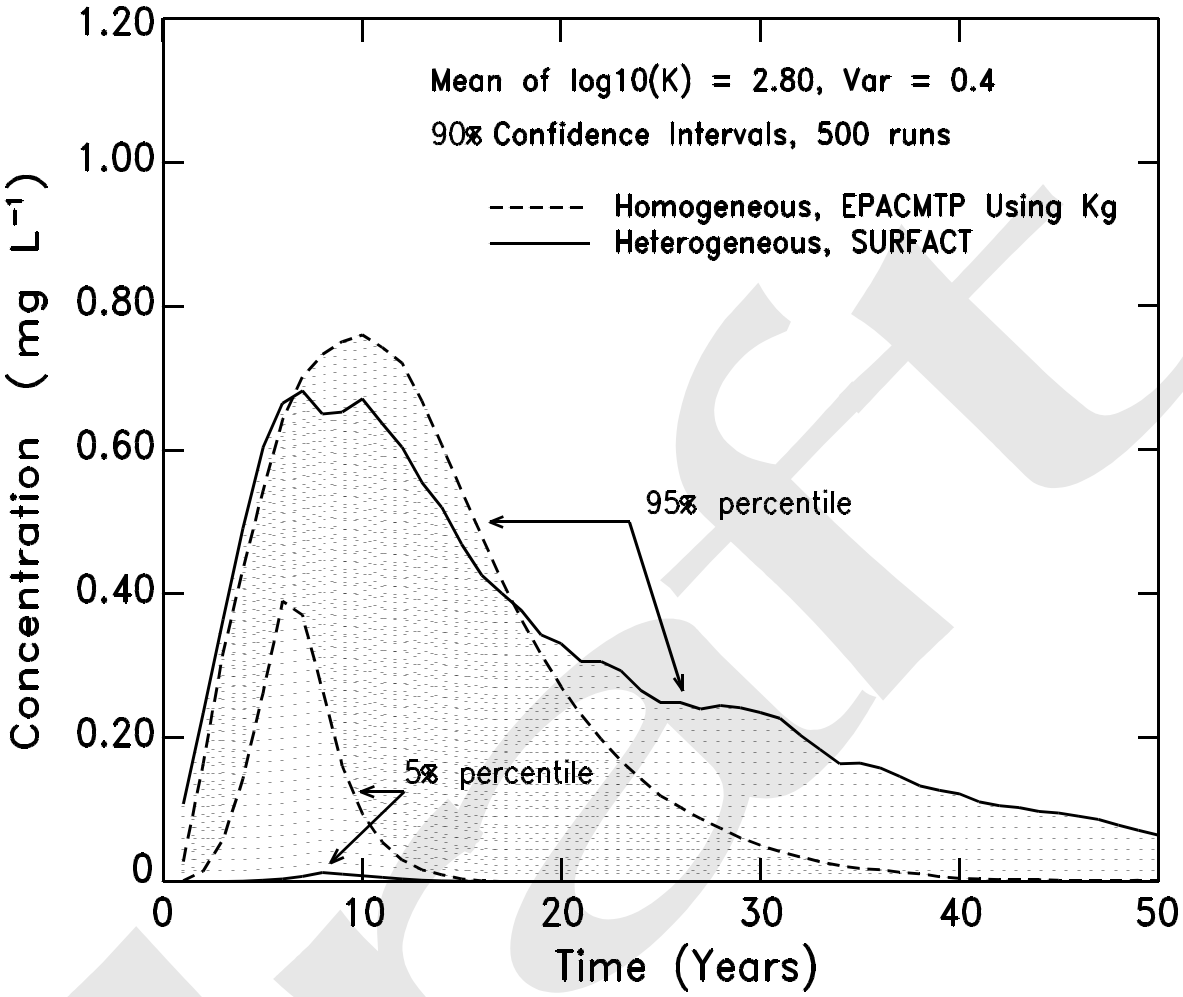

Figure 3.7 Comparison of Monte Carlo simulation results: homogeneous (EPACMTP) versus heterogeneous (MODFLOW-SURFACT.

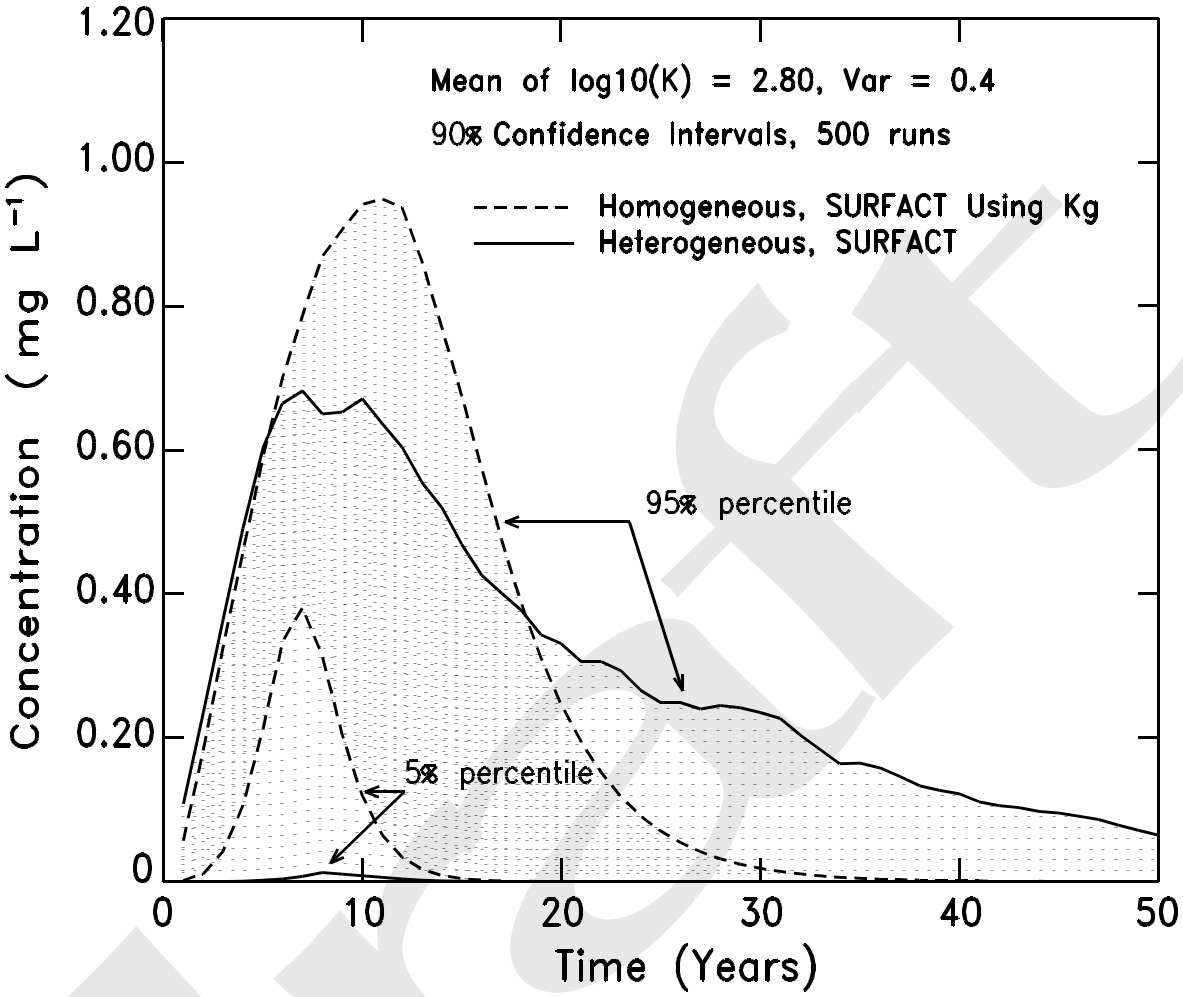

Figure 3.8 Comparison of Monte Carlo simulation results: homogeneous (MODFLOW-SURFACT) versus heterogeneous (MODFLOW-SURFACT).

to the one estimated from the heterogeneous model. The rough portion of the 95 percentile line for heterogeneous MODFLOW-SURFACT will become smooth when the number of Monte Carlo simulation increases.

The same results of the Monte Carlo simulation was presented in a different way using the cumulative probability approach (or the complementary cumulative distribution functions (CCDF)). In Figures 3.9 and 3.10, the probability of exceeding a certain concentration at the observation point was shown at selected times. For example, the Figure 3.9 suggest that, at 10 years for homogeneous EPACMTP case, there is about 85 percent probability that the concentration at the observation point will exceed 0.2 mg/L. At 30 years, the concentration will be less than 0.2 mg/L (i.e., probability of concentration exceeding 0.2 mg/L is almost zero). For the heterogeneous case (Figure 3.10), the probability that the concentration exceeding 0.20 mg/l at 10 years falls dramatically to about 40 percent from about 85 percent for the homogeneous case. Note that this trend was reversed at later times. At 20 and 30 years, the probabilities exceeding a certain concentration with the heterogeneous case were higher compared to the homogeneous case.

Conclusion

The impact of aquifer heterogeneity on contaminant transport was evaluated by comparing the computer simulation results on a hypothetical aquifer using homogeneous and heterogeneous hydraulic conductivities. For heterogeneous model simulations, two dimensional turning bands algorithm (TUBA) was used to generate the heterogeneous hydraulic conductivity. Transport of landfill leachate varied depending on the extent of heterogeneity of the conductivity. The degree of conductivity heterogeneity was, in turn, dependant on the TUBA input parameters such as the variance and spatial correlation of hydraulic conductivity. It was generally observed that, as the degree of hydraulic conductivity heterogeneity increases, the contaminant plumes exhibited greater spreading and the arrival time of the peak concentration at a selected point varies over a wider time frame. The relative magnitude of the simulated peak concentrations for the homogeneous and heterogeneous cases varied with the time of evolution. In earlier times, the peak concentration was larger in the homogeneous case, but in the heterogeneous case, the peak concentrations became larger in later times (although the absolute magnitudes of both concentrations were smaller compared to the earlier times).

Note that the findings in this study are based the statistical variation of one parameter, the hydraulic conductivity. Obviously, there are other hydrogeological and geochemical factors contributing to the aquifer heterogeneity. They will also have impact on the solute transport. These include porosity, dispersivity, sorption coefficient, and microbial degradation rates. Because the hydraulic conductivity is usually the major influencing parameter in the solute transport process, the heterogeneity of the hydraulic conductivity was the first one investigated in this study. It is postulated that the aquifer heterogeneity induced by the other parameters will follow a the similar pattern produced by the conductivity variation.

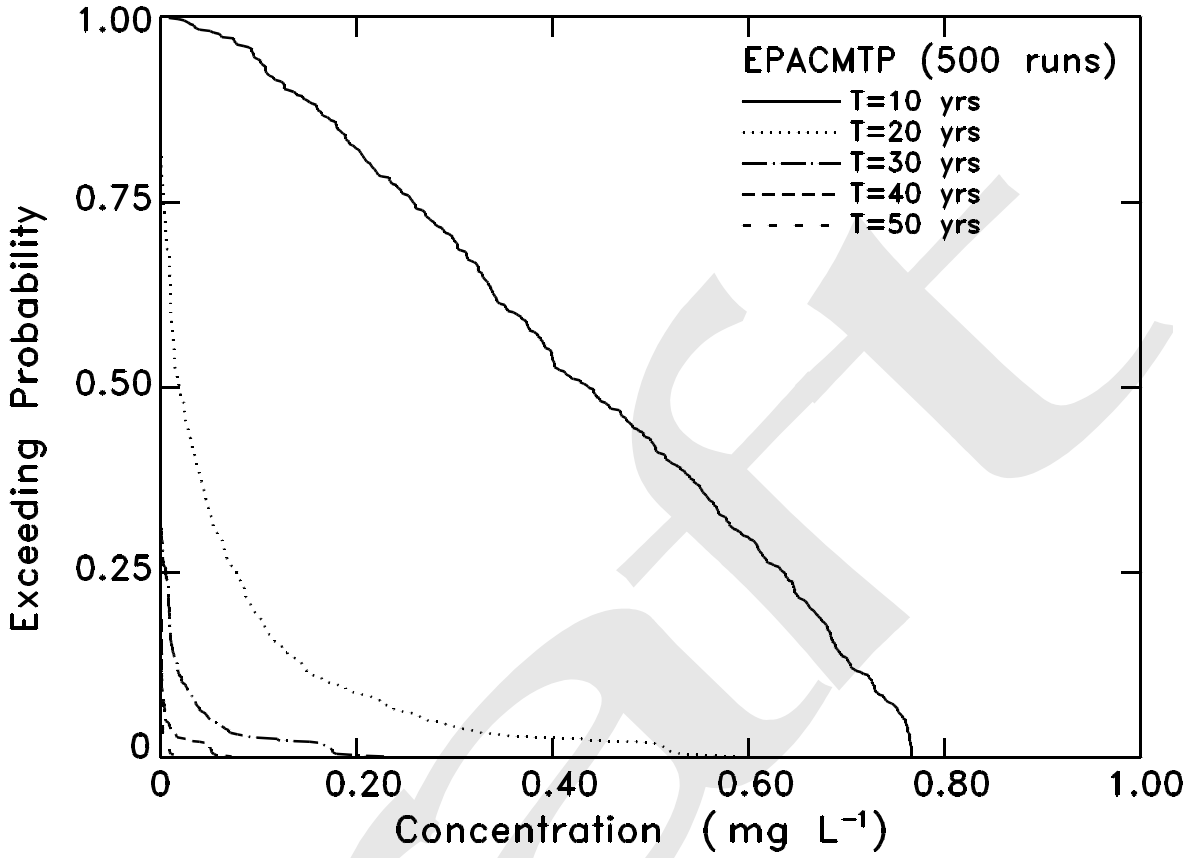

Figure 3.9 Cumulative distributions showing the probability of exceeding concentrations at the observation point (homogeneous EPACMTP run).

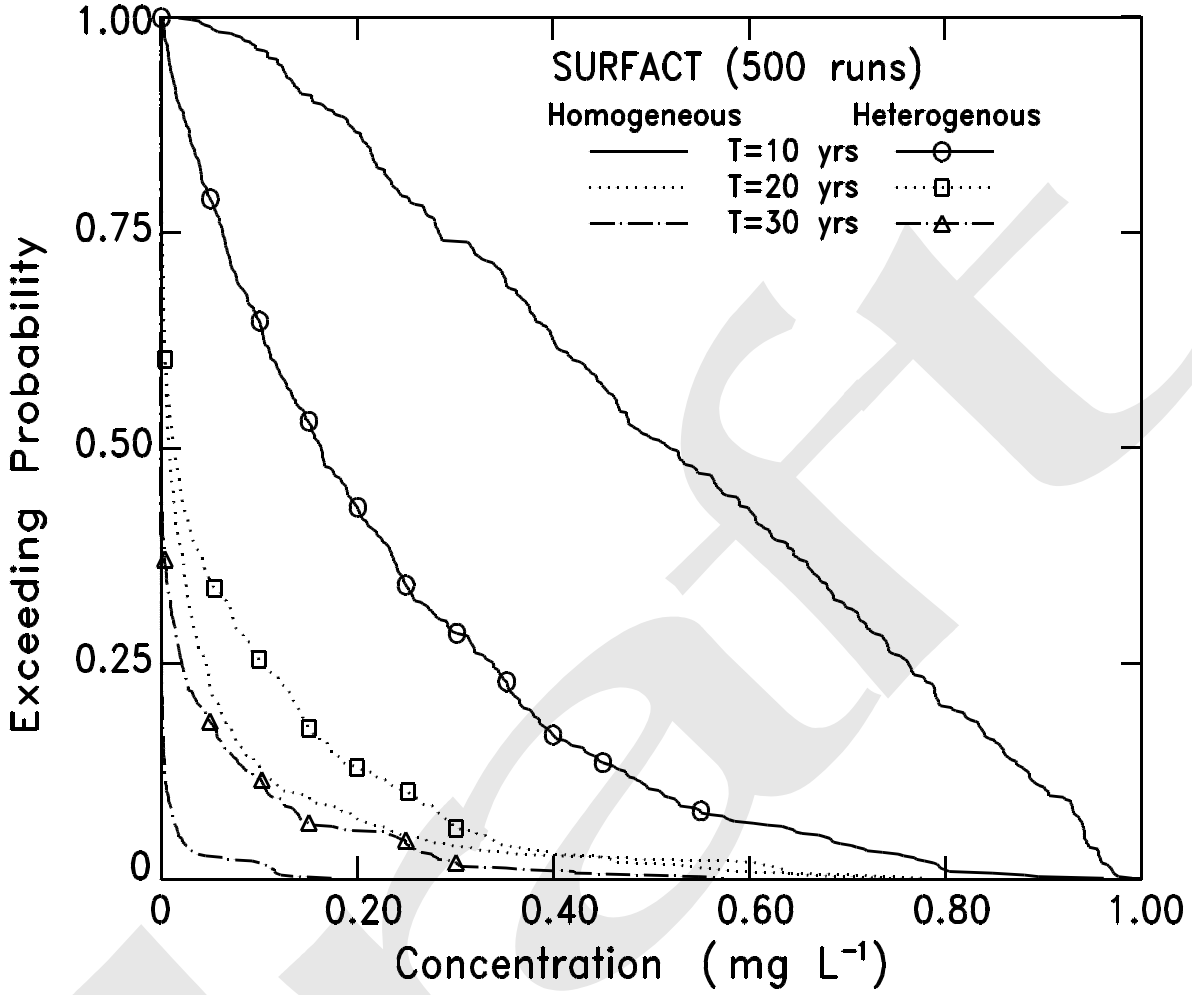

Figure 3.10 Comparison of exceeding probabilities at the times of 10, 20, and 30 years for homogeneous and heterogenous cases using MODFLOW-SURFACT.

References

API, 1989. Hydrogeologic Database for Groundwater Modeling. API Publication No. 4476, American Petroleum Institute.

Bredehoeft, John D., 1997. Fault Permeability near Yucca Mountain. Water Resources Research 33(11), pp.2459-2463.

Dagan, G. 1982. Stochastic modeling of groundwater flow by unconditional and conditional probabilities, 2, The solute transport. Water Resour. Res. 18(4):835-848.

Dagan, G. 1984 Solute transport in heterogeneous porous formations. J. Fluid Mech., 145:151-177.

Delhomme, J.O. 1976. Application de la theorie des variables regionalisees dans les sciences de l'eau. Ph.D. thesis, Univ. Pierre et Marie Curie, Paris, France.

El-Kadi, A.I. 1986. A computer program for generating two-dimensional fields of autocorrelated parameters. Ground Water 24(5):663-667.

EPA, 1986. Industrial Subtitle D Facility Study (called OPPI data), U.S. EPA, October 20, 1986.

EPA, 1987, DRASTIC: A Standardized System for Evaluating Ground Water Pollution Potential Using Hydrogeologic Settings, R.S. Kerr Env. Res. Lab., Ada, OK, EPA/600/2-87/036.

EPA, 1991. Regional Assessment of Aquifer Vulnerability and Sensitivity in the Conterminous United States, U.S. EPA Office of Solid Waste, Washington D.C., EPA/600/2-91/043.

EPA, 1996. EPA's Composite Model for Leachate Migration with Transformation Products (EPACMTP): Background Document. U.S. EPA Office of Solid Waste, Washington D.C. 20460

Fredericia, J., 1990. Saturated Hydraulic Conductivity of Clayey Tills and the Role of Fractures. Nordic Hydrology, 21:119-132.

Gburek, W.J. and J.B. Urban, 1990. The Shallow Weathered Fracture Layer in the Near-Stream Zone. Ground Water 28(6):875-883.

Goodrich, M.T., and J.T. McCord. 1995. Quantification of uncertainty in exposure assessments at hazardous waste sites. Ground Water, 33(5):727-732.

Gustafsson, E. and P. Anderson, 1991. Groundwater flow conditions in a low-angle fracture zone at Finnsjon, Sweden. Journal of Hydrology 126:79-111.

Heath, R.C., 1984, State Summaries of Groundwater Resources. U.S. Geological Survey Water-Supply Paper 2275.

Hsieh, P.A. and M. Shapiro, 1996. Hydraulic Characteristics of Fractured Bedrock Underlying the FSE Well Field at the Mirror Lake Site, Grafton County, New Hampshire. U.S. Geological Survey, Water-Resources Investigations Report 94-4015, 1:127-128.

Kaluarachchi, J. J. 1996. Effect of subsurface heterogeneity on free-product recovery from unconfined aquifers. J. Contaminant Hydrol. 22:19-37.

Kischinhevsky, M. and P.J. Paes-Leme, 1997. Modeling and Numerical Simulations of Contaminant Transport in Naturally Fractured Porous Media. Transport in Porous Media, 26:25-49.

Mantoglou, A., and J.L. Wilson. 1982. The turning bands method for simulation of random fields using line generation by a spectral method. Water Resour. Res. 18(5):1379-1394.

McKay, L.D., J.A. Cherry, and R.W. Gillham, 1993. Field Experiments in a Fractured Clay Till Hydraulic Conductivity and Fracture Aperture. Water Resources Research 29(4):1149-1162.

Mejia, J.M., and I. Rodriguez-Iturbe. 1974. On the synthesis of random field sampling from the spectrum: an application to the generation of hydrologic spatial processes. Water Resour. Res. 10(4):705-711.

NRC (National Research Council), 1996, Rock Fractures and Fluid Flow, Committee on Fracture Characterization and Fluid Flow, U.S. National Committee for Rock Mechanics, National Academy Press, Wash. D.C., pp. 551.

Odling, N.E., and I. Webman, 1991. A "Conductance" Mesh Approach to the Permeability of Natural and Simulated Fracture Patterns. Water Resources Research 27(10):2633-2643.

Ophori, D.U, T. Chan, and F.W. Stanchell, 1998. Hydrologic Response to Pumping and Contaminant Advection in a Fractured Rock Environment. J. of the American Water Resources Association 34(1), pp. 57-72.

Quinodoz, H.N.A., and A.L. Valocchi, 1993. Stochastic analysis of the transport of kinetically sorbing solutes in aquifers with randomly heterogeneous hydraulic conductivity. Water Resour. Res. 29(9):3227-3240.

Ray, C., T.R. Ellsworth, A.J. Valocchi, and C.W. Boast, 1997. An improved dual porosity model for chemical transport in macroporous soils. Journal of Hydrology, 193:270-292.

Schafer, G., and W. Kinzelbach, 1992. Stochastic modeling of in situ bioremediation in heterogeneous aquifers. J. Contaminant Hydrol. 10(1):47-73.

Shapiro, A.M., 1993. The Influence of Heterogeneity in Estimates of Regional Hydraulic Properties in Fractured Crystalline Rock. Memoires of the XXIVth Congress of IAH, AS, Oslo,

pp 125-136.

Sudicky, E.A. 1986. A natural gradient experiment on solute transport in a sand aquifer: spatial variability analysis of hydraulic conductivity and its role in the dispersion process. Water Resour. Res. 22:2069-2082.

Thackston, J., Y. Meeks, J. Stranberg, and H. Tuchfeld, 1989. Characterization of a Fracture Flow Groundwater System at a Waste Management Facility. Proc. of the Third National Outdoor Action Conference on Aquifer Restoration, Ground Water Monitoring and Geophysical Methods. May 22-25, 1989, National Water Well Association, pp.1079-1091.

Tompson, A.F.B., R. Ababou, and L.W. Gelhar. 1989. Implementation of the three-dimensional turning bands random field generator. Water Resour. Res. 25(10):2227-2243.

Valocchi, A.J. 1989. Nonequilibrium adsorption during reactive contaminant transport through heterogeneous aquifers. National Technical Information Service, PB91-136200, Springfield, VA. 43p.

Appendix A.

Fracture Assessment using the OPPI Database and Aquifer Vulnerability Report

APRIL 1, 1998

MEMORANDUM

Subject: Submittal of Draft Report on the HWIR Project

From: Sam Lee and Jin-Song Chen, Dynamac Corporation

To: Steve Schmelling and Joe Williams, USEPA

Please see the attached draft report on the ORD-OSW HWIR Science Plan project. All of your review comments were responded in this version. If you have any further questions, call me at (405) 436-6407.

Enclosure

Conference Call

Date:Sept. 3, 1998 (Thursday 1:00 pm, cst)

AttendeeZubair Saleem, OSW, USEPA

Steve Schmeeing and Joe Williams, NRMRL, USPEA

Sam Lee and Jin-Song Chen, Dynamac Corporation

Dua Guvanasen, Hydrogeologic Inc.

Agenda

1. Fracture Analysis

   1.1 Hydraulic Conductivity Increase for Fractures
   Proposed Range of K Increase
   Triangular Distribution of Weighting Function

   1.2 Additional Parameters Affecting Solute Transport in the Fractured Medium
   Porosity
   Dispersion and Diffusion
   Sorption
   Decay

2. Heterogeneous Aquifer

Fracture Analysis

1. Hydraulic Conductivity Increase in EPACMTP Simulation to Represent Fractured Media

Proposed Range of Hydraulic Conductivity Increase

The results of a limited literature survey (Table 2.4 of Dynamac's March 1998 report) indicated that the hydraulic conductivity of fractured media was increased by a factor of ten to thousands compared to non-fractured media. Note that ten out of eleven papers listed in the table contain actual measurements either from the field or laboratory.

The ranges of the hydraulic conductivity multiplier (ratio of the hydraulic conductivity representing fractured media to that of non-fractured media) are plotted in the Figure 1 which is a graphical presentation of the fourth column of the Table 2.4. In the figure, a new range of hydraulic conductivity variation for Monte Carlo simulation was determined based on the mean and standard deviation. The mean is an arithmetic average of representative values which were determined by taking mid-point in each multiplier ranges. Specifically, this range for the log of the ratio is mean (2.10) ± one standard deviation (0.93).

Triangular Distribution of Weighting Function

The log-transformed values of the multipliers are assumed to be in a triangular distribution. Using the triangular distribution function, it can be easily shown that 75% of the randomly generated multiplier values range from $10^{1.635} = 43$ to $10^{2.565} = 367$. In this case, the hydraulic conductivity for the fractured media will be increased by an average factor of 126($=10^{2.10}$) compared to the porous media.

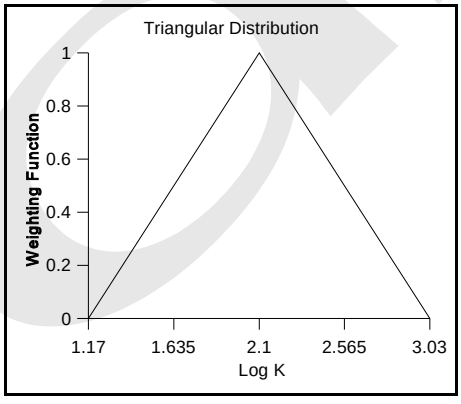

Although the literature survey is limited, the proposed range of the hydraulic conductivity multiplier is based on field and laboratory measurements. Therefore, additional Monte Carlo simulation using this new range is necessary. The new results should replace the preliminary simulation results in the draft report which were based on a lower range of hydraulic conductivity multipliers (from 1 to 100). Note that the initial range (1 to 100) was neither based on field measurement or a scientific literature survey. It was simply selected "to provide Hydrogeologic Inc. an initial framework to start modifying the EPACMTP source code."

1.2 Additional Parameters Affecting Solute Transport in the Fractured Medium

Most hydrogeologists agree that the hydraulic conductivity is the single most important and fundamental parameter in flow and transport simulation (Zheng and Bennett, 1995; USEPA, 1990), especially for passive or "near passive" contaminants. Movement of groundwater and contaminant is directly influenced by the hydraulic conductivity. Studies show that in most situations contaminant migration is advection dominated (USEPA, 1990).

However, there are also other physical and chemical parameters influencing groundwater flow and pollutant migration. These are porosity, dispersivity, sorption, and chemical reaction rates. To evaluate the relative impacts of these parameters on the contaminant migration, a one-dimensional transport equation is used for explanatory purpose:

$$R\frac{\partial C}{\partial t} = D\frac{\partial^2 C}{\partial x^2} - v\frac{\partial C}{\partial x} - \lambda RC\,,$$

where, $R = 1+(\rho_b K_d /n)$, ρ_b = bulk density, K_d = distribution coefficient, n = effective porosity, C = contaminant concentration, t = time, D = Dispersion coefficient (= $\alpha_L q/n$), α_L = dispersivity, q = Darcy velocity, x = length, v = seepage velocity (= q/n), λ = decay rate constant.

Porosity

In the above transport equation, seepage velocity is a function of hydraulic conductivity (K) and, in turn, K is function of fluid and soil properties (Freeze & Cherry, 1979). For granular material, we have:

$$K = \frac{Bd^2\rho g}{\mu},$$

where, B = proportionality constant, d = size of soil particle, ρ = fluid density, g = graviational constant, μ = fluid viscosity.

The proportionality constant B is related to porosity through *the Kozeny-Carmen equation* (Bear, 1972)

$$K = (\frac{\rho g}{\mu})[\frac{n^3}{(1-n^2)}](\frac{d^2}{180})$$

As shown in the above equation, hydraulic conductivity is emperically related to the porosity and the size of soil particles, as well as and fluid properties. Considering the fact that soil sizes vary over much larger range than the variation of porosity, hydraulic conductivity variation is largely dependent on the size of soil particles rather than porosity. Subsequently, although seepage velocity is a function of both hydraulic conductivity and porosity (and hydraulic gradient), the variation of hydraulic conductivity has a much greater impact on seepage velocity than that of porosity. Ranges of hydraulic conductivity and porosity for various geologic materials are summarized in Tables 1 and 2.

For a set of planar fractures, an equivalent hydraulic conductivity may be calculated with an equation developed by Snow (1968)

$$K = \frac{\rho g}{\mu}\frac{Nb^3}{12} = \frac{\rho g}{\mu}\frac{n_f b^2}{12}$$

where n_f is the fracture porosity, b is the aperture. The fracture porosity n_f is the product of N and b, where N is the number of joints per unit distance across of the face of the rock (L^{-1}). In this case, the equivalent conductivity, K, is linearly proportional to the product of the fracture porosity and the square of the fracture aperture.

Dispersion

Researchers (Gelhar and Axness, 1983; Dagan, 1982, 1984, 1988; Neuman et al., 1987) used stochastic transport theories to relate the macrodispersion to the statistical properties of hydraulic conductivity, which leads to enhanced spreading of solutes in groundwater,. In these approaches, the variance and spatial correlation of the log K distribution are necessary to determine the magnitude of dispersion. The higher spatial variability of hydraulic conductivity in the aquifer will result in higher variability in the velocity field, which, in turn, leads to increased dispersive mixing and spreading of the solutes. Since the details of these approaches are beyond scope of this study these are omitted here.

Gelhar et al. (1992) collected field data to show another property of dispersivity: it generally appears to be dependent on the scale of contaminant transport (Figures 2 and 3). Figure 3 suggests that these data are more representative for local to intermediate scales with respect to data reliability. Note that the receptor well locations in EPACMTP's

database (OPPI data) are generally close to the small or intermediate scales in these figures. Figure 3 shows that the longitudinal dispersivity for these scales varies over two or four orders of magnitude while the hydraulic conductivity values in Table 1 tend to vary up to 12 orders of magnitude. In addition, remembering the fact that contaminant transport tends to be generally advection dominant, impact due to dispersivity could be considered as smaller than that of the hydraulic conductivity. As customary as it has been in the subsurface modeling, the dispersivity value is varied to adjust the model output in calibration process.

Sorption and Decay Rate

Linear sorption is dependent on soil organic carbon content and type of chemicals in the contaminant. Decay rate is largely chemical dependent. To my knowledge, no field investigation has been reported showing that the sorption coefficient or decay rate in porous media is different than that in the fractured media. If a difference exists between the two medium, its impact on the contaminant transport would likely be smaller than that due to the hydraulic conductivity.

Heterogeneity of Aquifer Hydraulic Conductivity

Several research papers dealing with actual field aquifer heterogeneity data were reviewed and summarized here. Dillard et al. (1997) analyzed more than 600 permeability estimations at a crude-oil spill site near Bemidji, Minnesota. The two predominant lithologies at the site are: coarse glacial outwash deposit and fine-grained interbedded lenses. The mean, variance, minimum, and maximum of the distribution obtained using the 613 log permeability (log *k* in square centimeters) estimates are –7.24, 0.25, -9.74, and –6.03, respectively (see Table 3 below). Similar results at the same site was previously reported by Essaid et al. (1993) from particle size distribution.

In an uncertainty analysis for subsurface contaminant transport simulation, James and Oldenburg (1997) used actual site data, in which the range of permeability was from 10^{-8} to 10^{-4} cm^2 and variance was 0.5. The lithology at the site consists of interbedded layers of clay, silt, and sand comprising a thick vadose zone. Hess at al. (1992) conducted a hydraulic conductivity variability study in medium-to-coarse sand and gravel aquifer on Cape Cod, MA to reveal smaller variances (0.14 and 0.24). Except for the two papers in Table 3 (Hufshmeid, 1986 and Rehfeldt et al., 1992), all the study indicate that the estimated variances are less than or equal to 0.5. Note that the variance value of 2.15 in Hufshmeid (1986) was based on the natural logarithm (base e). The value of 4.5 in Rehfeldt et al. (1992) was the spatial covariance value which is different from the ones in

the other papers.

Degree of aquifer heterogeneity is dependent on the variance of hydraulic conductivity. A high variance will produce a wide range of hydraulic conductivity variation and higher aquifer heterogeneity whereas a low variance will produce less heterogenous (more homogeneous) fields. Note that the variance of 0.4 used in the section 3 of the draft report to generate heterogeneous hydraulic conductivity distribution (using TUBA) is within the range of variance values summarized in the Table 3.

References

Ayers, J.F., X. Chen, and D.C. Gosselin, 1998, Behavior of nitrate-nitrogen movement around a pumping high-capacity well: A field example, Ground Water, 36(2), p. 325-337.

Bakr, A.A., Effect of spatial variations of hydraulic conductivity on groundwater flow, Ph.D. dissertation, N.M. Inst. Of Min. & Technol., Socorro, 1976.

Bear, J., 1972, Dynamics of Fluids in Porous Media, American Elsevier, NY, 764 p.

Bjerg, P.L., K.Hinsby, T.H. Christensen, & P. Gravesen, 1992, Spatial variability of hydraulic conductivity of an unconfined sandy aquifer determined by a mini slug test, J. of Hydrology, 136, p. 107-122.

Bradbury, K.R. & R.W. Taylor, 1984, Determination of the hydrogeologic properties of lakebeds using offshore geophysical surveys, Ground Water, 22(6), p. 690-695.

Bradbury, K.R., E.R. & Rothschild, 1985, A computerized technique for estimating the hydraulic conductivity of aquifers from specific capacity data, Ground Water, 23(2), p. 240-246.

Capuano, R.M. & R.Z. Jan, 1996, In Situ hydraulic conductivity of clay and silty-clay fluvial-deltaic sediments, Texas Gulf Coast, Ground Water 34(3), p. 545-551.

Cho, J.S., J.T. Wilson, D.C. DiGiulio, J.A. Vardy, and W. Choi, 1997, Implementation of natural attenuation at a JP-4 jet fuel release after active remediation, Bioremediation 8: p.265-273.

Cravens, S.J. and L.C. Ruedisili, 1987, Water movement in till of East-Central South Dakoda, Ground Water, 25(5), p. 555-561.

Dillard, L.A., H.I. Essaid, and W.N. Herkelrath, 1997, Multiphase flow modeling of a crude-oil spill site with a bimodal permeability distribution, Water Resour. Res., 33(7), p. 1617-1632.

Essaid, H.I., W.N. Herkelrath, and K.M. Hess, 1993, Simulation of fluid distributions observed at a crude oil spill site incorporating hydteresis, oil entrapment, and spatial variability of hydraulic properties, Water Resour. Res., 29(6), p. 1753-1770.

Freeze, R. and J. A. Cherry, Groundwater, 1979, Prectice-Hall, Englewood, NJ, 604 p.

Gelhar, L.W., C. Welty, and K.W. Rehfeldt, 1992, A Critical review of data on field-scale dispersion in aquifers, Water Resour. Res., 28(7), p. 1955-1974.

Harman, J., W.D. Robertson, J.A. Cherry, & L. Zanini, 1996, Impacts on a sand aquifer from an old septic system: Nitrate and Phosphate, Ground Water, 34(6), p. 1105-1114.

Hess, K.M., S.H. Wolf, and M.A. Celia, 1992, Large-scale natural gradient tracer test in sand and gravel, Cape Cod, Massachusetts, 3. Hydraulic conductivity variability and calculated macrodispersivities, Water Resour. Res., 28(8), p. 2011-2027.

Hill, B.M., 1996, Use of numerical model for management of shallow ground-water levels in the Yuma, Arizona area, Ground Water, 34(3), p. 397-404.

Hill, B.M., 1993, Hydrogeology, numerical model and scenario simulations of the Yuma area groundwater flow model, Arizona, California and Mexico. Arizona Dept of Water Resources - Hydrology Division, Modeling Report No. 7. 113p.

Hufschmied, P., 1986, Estimation of three-dimensional statistically anisotropic hydraulic conductivity field by means of single well pumping tests combined with flowmeter measurements, Hydrogeologie, 2, p. 163 – 174.

Istok, J.D., C.A. Rautman, L.E. Flint, & A.L. Flint, 1994, Spatial variability in hydrologic properties of a volcanic tuff, Ground Water, 32(5), p. 751-760.

James, A.L. and C.M. Oldenburg, 1997, Linear and Monte Carlo uncertainty analysis for subsurface contaminant transport simulation, Water Resour. Res., 33(11), p. 2495-2508.

Kehew, A.E., W.T. Straw, W.K. Steinmann, P.G. Barrese, G. Passarella, & W.S. Peng, 1996, Ground-water quality and flow in a shallow glaciofluvial aquifer impacted by agricultural contamination, Ground Water, 34(3), p.491-500.

Killey, R.W.D. & G.L. Moltyaner, 1988, Twin lake tracer tests: Setting, methodology, and hydraulic conductivity distribution, Water Resour Res, 24(10), p. 1585-1612.

Mackay, D.M., D.L. Freyberg, P.V. Roberts, and J.A. Cherry, 1986, A Natural gradient experiment on soulte transport in a sand aquifer, 1. Approach and overview of plume movement, Water Resour. Res., 22(13), p. 2017-2029.

Mas-Pla, J., T.C.J. Yeh, T.M. Williams, and J.F. McCarthy, 1997, Analysis of slug tests and hydraulic conductivity variations in the near field of a two-well tracer experiment site, Ground Water 35(3), p. 492-501.

McCloskey, T.F. and E.J. Finnemore, 1996, Estimating hydraulic conductivities in an alluvial basin from sediment facies methods, Ground Water, 34(6), p. 1024-1032.

Norris, S.E., Aquifer tests and well field performance, Scioto River Valley, Ohio: Part I, Ground Water, 21(3), p.287-292.

Pickens, J.F. and G.E. Grisak, 1981, Scale-dependent dispersion in a stratified granular aquifer, Water Resour. Res., 17(4), p. 1191-1211.

Prudic, D., 1982, Hydraulic conductivity of a fine-grained till, Cattaraugus County, New York, Ground Water, 20(2), p. 194-204.

Rehfeldt, K.R., J.M. Boggs, and L.W. Gelhar, 1992, Field study of dispersion in a Heterogeneous aquifer, 3. Geostatistical analysis of hydraulic conductivity, Water Resour. Res., 28(12), p. 3309-3324.

Rovey, C.W. & D.S. Cherkauer, 1994, Relation between hydraulic conductivity and texture in a carbonate aquifer: Regional continuity, Ground Water, 32(2), p.227-238.

Scholl M.A. and S. Christenson, 1998, Spatial variation in hydraulic conductivity determined by slug tests in the Canadian River Alluvium near the Norman Landfill, Norman, Oklahoma, USGS, Water-Resources Investigations Report 97-4292.

Shapiro, A.M. & P.A. Hsieh, 1998, How good are estimates of transmissivity from slug tests in fractured rock?, Ground Water 36(1), p. 37-48.

Simpkins, W.W., K.R. Bradbury, and D.M. Mickelson, 1989, Methods for evaluating large-scale heterogeneity in fine-grained glacial sediment, Proc. of the conference on new field techniques for quantifying the physical and chemical properties of heterogeneous aquifers, March 20-23, 1989, Dallas, TX, National Water Well Assoc., Dublin, OH.

Smith, R.T. and R.W. Ritzi, 1993, Designing a nitrate monitoring program in a heterogeneous, carbonate aquifer, Ground Water, 31(4), p. 576-584.

Snow, D.T., 1968, Rock fracture spacings, openings, and porosities, J. Soil Mech., Found Div., Proc. Amer. Soc. Civil Engrs., v. 94, p. 73-91.

Storck, P., J.W. Eheart, and A.J. Valocchi, 1997, A method for the optimal location of monitoring wells for detection of groundwater contamination in three-dimensional heterogenous aquifers, Water Resour. Res., 33(9), p. 2081-2088.

Sudicky, E.A., 1986, A natural gradient experiment on solute transport in a sand aquifer: Spatial variability of hydraulic conductivity and its role in the dispersion process, Water Resour. Res., 22(13), p. 2069-2082.

Taffet, M.J., J.A. Oberdorfer, W.A. McIlvride, 1989, Remedial investigation and feasibility study for the Lawrence Livermore National Laboratory Site 300 Pit 7 Complex, Lawrence Livermore National Lab, Livermore, CA.

Temples, T.J. & M.G.Waddell, 1996, Application of petroleum geohpysical well logging and sampling techniques for evaluating aquifer characteristics, Ground Water, 34(3), 523-531.

Tompson, A.F.B., 1990, Flow and transport within the saturated zone beneath Lawrence Livermore National Laboratory: Modeling considerations for heterogeneous media, Lawrence Livermore National Lab, Livermore, CA.

Tompson, A.F.B., R.D. Falgout, S.G. Smith, W.J. Bosl, & F. Ashby, 1998, Analysis of subsurface contaminant migration and remediation using high performance computing, Water Resour. Res., Accepted for publication.

Urban, J.B., and W.J., Gburek, 1988, Determination of aquifer parameters at a ground-water recharge site, Ground Water 26(1), p. 39-53

USEPA, 1990, A New Approach and Methodologies for Characterizing the Hydrogeologic Properties of Aquifers, EPA/600/2-90/002, R.S. Kerr Res. Lab., Ada, OK.

Way, S.C. & C.R. 1982, McKee, In-situ determination of three-dimensional aquifer permeabilities, Ground Water, 20(5), p.594-603.

Wolf, S.H., M.A. Celia, and K.M. Hess, 1991, Evaluation of Hydraulic Conductivities Calculated from Multiport-Permeameter Measurements, Ground Water, 29(4), 516-525.

Xiang, J., 1996, Evaluation of hydraulic conductivity of Carson County well field, Amarillo, Texas, Ground Water, 34(6), p. 1042-1049.

Young, S.C. and H.S. Pearson, 1990, Characterization of a three-dimensional hydraulic conductivity field with an electromagnetic borehole flowmeter, Proc of 4th National outdoor action conference, Las Vegas, NV, May 14-17, 1990, Ground Water Management, Dublin, OH, p. 83-97.

Young, S.C., 1995, Characterization of high-K pathways by borehole flowmeter and

tracer tests, Ground Water, 33(2), p. 311-318.

Zhang, Z. and M.L. Brusseau, 1998, Characterizing three-dimensional hydraulic conductivity distributions using qualitative and quantitative geologic borehole data: Application to a filed site, Ground Water, 36(4), p. 671-678

Zheng, C. and D. B. Gordon, 1995, Applied Contaminant Transport Modeling, Van Nostrand Reinhold, 440 p.

Table 1. Range of Hydraulic Conductivity for Various Rock Types

Material	Hydraulic conductivity (m/sec)
Sedimentary	
Gravel	3×10^{-4} to 3×10^{-2}
Coarse sand	9×10^{-7} to 6×10^{-3}
Medium sand	9×10^{-7} to 5×10^{-4}
Fine sand	2×10^{-7} to 2×10^{-4}
Silt, loess	1×10^{-9} to 2×10^{-5}
Till	1×10^{-12} to 2×10^{-6}
Clay	1×10^{-11} to 5×10^{-9}
Unweathered marine clay	8×10^{-13} to 2×10^{-9}
Sedimentary rocks	
Karst and reef limestone	1×10^{-6} to 2×10^{-2}
Limestone, dolomite	1×10^{-9} to 6×10^{-6}
Sandstone	3×10^{-10} to 6×10^{-6}
Siltstone	1×10^{-11} to 1×10^{-8}
Salt	1×10^{-12} to 1×10^{-10}
Anhydrite	4×10^{-13} to 2×10^{-8}
Shale	1×10^{-13} to 2×10^{-9}
Crystalline rocks	
Permeable basalt	4×10^{-7} to 2×10^{-2}
Fractured igneous and metamorphic rock	8×10^{-9} to 3×10^{-4}
Weathered granite	3×10^{-6} to 5×10^{-5}
Weathered gabbro	6×10^{-7} to 4×10^{-6}
Basalt	2×10^{-11} to 4×10^{-7}
Unfractured igneous and metamorphic rocks	3×10^{-14} to 2×10^{-10}

Source: Zheng and Bennett, 1995

TABLE 2 Values of Porosity for Various Geologic Materials

Material	Porosity (%)
Sedimentary	
Gravel, coarse	24-36
Gravel, fine	25-38
Sand, coarse	31-46
Sand, fine	26-53
Silt	34-61
Clay	34-60
Sedimentary rocks	
Sandstone	5-30
Siltstone	21-41
Limestone, dolomite	0-20
Karst limestone	5-50
Shale	0-10
Crystalline rocks	
Fractured crystalline rocks	0-10
Dense crystalline rocks	0-5
Basalt	3-35
Weathered granite	34-57
Weathered gabbro	42-45

Source: Zheng and Bennett, 1995

Table 3. Distribution of hydraulic conductivity values from selected papers.

	Reference & Site Name	Aquifer Material	# of Test	Size of Test Zone	Estimation Method	Log of Hydraulic Conductivity or Permeability				Variance of Log (H/P)
						H/P[4]	Mean	Min	Max	
1	Bakr, A.A. (1976), Mt. Simon, Northeastern IL	sandstone	193 233 213 164 303 161 149 217	193 ft thick 233 ft thick 213 ft thick 164 ft thick 303 ft thick 161 ft thick 149 ft thick 217 ft thick	Lab core analysis (K_h)	H	0.89 1.21 1.38 1.22 0.79 0.52 0.67 0.63			0.90 0.53 0.60 0.47 0.67 0.77 0.81 0.71
		Arithmetic Average	204	204		H	0.93			0.68
		sandstone	193 233 213 164 303 161 149 217	193 ft thick 233 ft thick 213 ft thick 164 ft thick 303 ft thick 161 ft thick 149 ft thick 217 ft thick	Lab core analysis (K_v)	H	0.63 1.02 1.22 0.97 0.61 0.11 0.33 0.33			0.76 0.60 0.61 0.45 0.63 0.59 0.64 0.72
		Arithmetic Average	204	204		H	0.67			0.63
2	Pickens & Grisak (1981), Perch Lake Basin, Canada	glaciofluvial, sand aquifer	19 17	11 m thick	Tracer test (one well) Tracer test (two wells)	H	-0.4 -0.24			0.48 0.09
3	Prudic (1982), Western New York	fine-grained till	20 20 14 6 7	250 x 400 m 15 m thick	Slug test (Hvorslev) Slug test (Cooper) Permeameter Consolidation test Mercury Porosimeter	H	-7.10 -6.64 -7.13 -7.40 -7.55	-8.00 -7.40 -7.68 -7.96 -8.00	-5.00 -4.40 -6.12 -7.03 -7.10	0.90 0.90 0.27 0.18 0.14

4	Way & McKee (1982), Sweetwater County, WY		fluvial sandstone & claystone	8	120 x 250 m 75 m thick	Pump test	H	-3.80	-3.97	-3.65	0.01
5	Norris (1983), Scioto River Valley, OH		sand & gravel outwash	13	7 miles long 40 - 65 ft thick	Pump test	H	-0.80	-1.00	-0.62	0.01
6	Bradbury & Taylor (1984), Lake Michigan Shore, WI	Peninsula site	glacial till & lake clay (aquitard)	8	3 x 4 miles 1 - 68 ft thick	Geophysical method (electrical resistivity) (K_v)	H	-4.61	-5.80	-2.29	1.04
		Point Beach	clay till (aquitard)	7	1 x 2 miles 60-130 ft thick			-7.26	-7.29	-7.24	0.003
		Mequon site	glacial till (aquitard)	4	40 - 70 ft thick			-6.24	-7.26	-5.34	0.62
7	Bradbury & Rothschild (1985), Wisconsin	Peninsula site	fractured dolomite aquifer	223	18 mi^2	Specific capacity test	H	-2.62			0.37
		Central sand plain of WI	sandy glacial outwash aquifer	266	612mi^2			-1.19			0.06
8	Mackay et al. (1986) Borden, Ontario, Canada		fine- to medium-grained sand aquifer	26	100 x 120 m 9 m thick	Slug test	H	-2.15	-2.30	-1.70	----
9	Sudicky (1986) Borden, Ontario, Canada		fine- to medium-grained sand aquifer	1279	13 & 20m long 2.5-4.5 m thick	Permeameter (core test)	H	-2.14	-2.30	-1.70	0.07
10	Hufshmied (1986), Aefligen, Switzerland		coarse gravel aquifer	307	20 m thick	Flowmeter (16 wells)	H	-0.22			0.41
11	Cravens & Ruedisili (1987), East-central SD		weathered till aquifer unweathered till aqfr	26 35	50x50 miles 7-17 m thick	Slug test	H	-6.15 -7.26	-7.75 -8.75	-4.25 -5.25	0.86 0.77

12	Urban & Gburek (1988), Willow Grove, PA	sandstone aquifer & shale	12 17 8 13 7	230x130 m 0.7-12 m thick	Grain size analysis pump test ground water contour slug test recharge mound	H	-4.48 -3.15 -4.26 -3.39 -3.09	-4.56 -3.54 -4.57 -4.25 -3.34	-4.30 -2.53 -3.07 -2.53 -2.67	0.004 0.08 0.25 0.34 0.05
13	Killey & Moltyaner (1988), Twin Lake, NW of Ottawa, Canada	fluvial sand	53 22 8 91 89	500 x 300 m 10 m thick	Permeameter (K_v) Borehole dilution Slug test (Hvorslev) Grain size analysis Tracer test	H	-1.86 -1.86 -2.18 -1.90 -1.69	-1.97	-1.37	0.04 0.03 0.06 0.005 0.01
14	Simpkins et al. (1989), Southeastern WI	till sediment	32 29	35 x 25 Km 100m thick	Slug test Lab test	H	-6.52 -9.00			0.71 0.04
15	Taffet et al. (1989), San Joaquin County, CA	alluvial deposit	33	300 x 500 m 6 m thick	Pump & slug tests	H	-3.87	-5.52	-2.14	0.63
16	Tompson (1990), Livermore, CA	alluvial deposit: silt, sand & gravel	167	1.5 x 3 Km 100 m thick	Pump & slug tests	H	-2.85	-5.33	-1.03	0.60
17	Young & Pearson (1990) & Young (1995), Columbus AFB, MS	fluvial deposit sandy gravel	881	1 ha 10 m thick	Flowmeter	H	-1.49	-5.1	-0.20	0.92

18	Wolf et al. (1991) Otis Air Base, Cape Cod, MA	glacial outwash (sand & gravel)	33 33 33 83 53	single borehole over 9 m thickness	Permeameter (repacked) Krumbein-Monk[3] Hazen[2] Permeameter Flowmeter	H	-1.43 -1.39 -1.41 -1.43 -0.92			0.05 0.05 0.04 0.04 0.02
19	Bjerg et al. (1992), Western Denmark	glacial outwash sandy aquifer	244	50 x 200 m 5 m thick	Slug test	H	-1.30	-2.10	-0.65	0.07
20	Hess et al.(1992) Otis Air Base, Cape Cod, MA	glacial outwash (sand & gravel)	668 825	20 x 50 m 8 m thick	Flowmeter Permeameter	H	-0.96 -1.46	-1.89 -2.22	-0.43 -0.85	0.05 0.03
21	Rehfeldt et al.(1992), Columbus AFB, MS	alluvial aquifer	2187 214 22 87 6200	400 x 600 m 10 m thick	Flowmeter Grain size Slug test Permeameter Facies mapping	H	-2.26 -1.35 -1.78 -4.21 -1.39	-4.39 -2.91 -3.17 -6.51 -6.99	0.17 1.39 -0.74 -2.00 2.00	0.85 0.58 0.34 1.04 0.09
22	Smith & Ritzi (1993), Dayton, OH	fractured carbonate aquifer	21	1 x 2 km 20 m thick	Slug test (Cooper) Slug test (Bower &Rice) Slug test (Widdowson)	H	-3.53 -3.62 -3.52	-5.15 -5.25 -5.12	-2.44 -2.64 -2.57	0.74 0.57 0.59
23	Essaid et al. (1993) Bemidji, MN	glacial outwash	146	7 boreholes from 120 x 4m transect	Kozeny-Carmen[1] Hazen[2] Krumbein-Monk[3]	P	-6.12 -6.68 -6.55	-6.85 -8.33 -8.17	-5.15 -6.24 -6.07	0.07 0.06 0.07

24	Istok et al. (1994), Yucca Mountain, NV		volcanic ash flow tuff	120 133 33 286	upper ash layer lower ash layer pumice layer Entire Base	Lab core test Core samples from a 1.3 Km long and 40 m thick transect	H	-4.73 -1.83 0.86 -2.93	-6.8 -4.9 -2.5 -6.8	-1.1 -0.2 1.6 1.6	1.58 1.00 0.50 3.61
25	Rovey & Cherkauer (1994) dolomite aquifer (carbonate aquifer over 3500 Km^2)	Haven, WI	wathered zone mudstone mudstone	35 51 82	140 m thick	Injection-pressure test	H	-4.15 -5.30 -4.0			0.40 0.30 0.30
		Ozaukee County, WI	mudstone mudstone mudstone/packstone	15 10 6	150 m thick	Injection-pressure test	H	-4.10 -4.60 -3.49			0.31 1.21 0.62
		Milwaukee County, WI	wathered zone mudstone packstone mudstone mudstone/packstone	17 123 17 23 11	100 m thick	Injection-pressure test	H	-3.80 -5.77 -3.89 -5.89 -3.92			0.53 1.96 0.55 1.00 0.23
		Chicago, IL	mudstone packstone mudstone mudstone/packstone	49 27 34 45	100 m thick	injection-pressure test	H	-6.30 -5.05 -5.70 -6.70			0.74 1.00 0.88 0.27
		Chicago, IL	wathered zone mudstone/packstone	13 27	50 m thick	injection-pressure test	H	-3.70 -5.22			2.25 1.00
26	Capuano & Jan (1996), Galveston County, TX		Caly & silty-clay	16 16	2 wells 8 m thick	pump test (Theis curve) pump test (Time drawdoun)	H	-2.46 -2.50	-2.54 -2.62	-1.98 -1.87	0.02 0.03

27	Harman et al. (1996), Ontario, Canada	sand unconfined aquifer	135	120 x 8 m transect	Hazen[(2)] & permea meter test	H	-1.74	-1.98	-1.52	0.01
28	Hill (1996), Yuma, AZ based on Hill (1993)	fluvial & deltaic sediments	30	20 x 20 miles 20-40 ft thick	pump test	H	-1.23	-1.75	-0.75	0.07
29	Kehew et al. (1996), Southwestern Michigan	glaciofluvial deposit sand & gravel	10	20 x 23 Km 76 m thick	slug test	H	-1.97	-3.39	-1.24	0.53
30	McCloskey & Finnemore (1996), San Jose, CA	alluvial basin sand & gravel	56	12 x 4 Km 100 m thick	11 pump tests 45 specific capacity tests	H	-1.74	-3.25	-0.62	0.55
31	Temples & Waddell (1996), Hilton Head Island, SC	sand & clay	28	single well of 3800 ft thick	Geophy sical well log (2806 - 3740 ft thicknes s)	H	-2.34	-2.80	-2.14	0.02
32	Xiang (1996), Amarillo, TX	sand, gravel & clay	11	4 x 4 Km 160 m thick	pump test: Theis Cooper & Jacob Neuma n	H	-2.04 -2.04 -2.40	-2.44 -2.44 -2.59	-1.61 -1.61 -2.22	0.06 0.06 0.02
33	Cho et al. (1997) Elizabeth City, NC	flood plain sand	46	34 x 10 m transect	Geopro be	H	-2.95	-4.19	-2.00	0.49
34	Dillard et al.(1997) Bemidji, MN	glacial outwash	269	100 x 140 m 10 m thick	Krumbe in-Monk[(3)]	P	-7.24	-9.74	-6.03	0.25

35	Mas-Pla et al. (1997) Georgetown, SC	loamy sand & gleyed sand	248 248 229	5 x 5 m 3 m thick	slug test: Hvorslev Bouwer & Rice Cooper et al.	H	-2.78 -2.87 -2.96	-4.01 -4.13 -5.08	-1.86 -1.83 -1.09	0.26 0.31 1.05
36	Stork et al.(1997), Will County, IL	silty clay & minor gravel	?	900 x 600 m 10 m thick	permeameter & others ?	H	-3.0			0.09
37	Ayers et al. (1998), Platte River valley, NE	sand & gravel	41	40 x 40 m 10 m thick	Hazen	H	-0.87	-1.21	-0.17	0.04
38	Scholl & Christenson (1998), Norman Landfill, OK	alluvial	40	215 x 10 m transect	Slug Test	H	-2.23	-4.08	-1.55	0.27
39	Shapiro & Hsieh (1998) Central New Hampshire	glacial drift with fractured rock	14 13	100 x 100 m 10 - 140 m thick	fluid injection test slug test	H	-5.48 -5.20	-8.37 -6.90	-3.81 -3.22	1.39 1.04
40	Tompson et al. (1998) Livermore, CA	alluvial deposit	240	3.8 x 3.8 Km 100 m thick	pump, slug, and core tests	H	-2.93			0.34
41	Zhang & Brusseau (1998), Tucson, AZ	sand: lower 15 m thick sand: upper 20 m thick sand: upper 11 m thick	21 81 29	4 x 4 Km	pump test pump test Lab core test	H	-2.99 -1.81 -4.74	-3.75 -3.75 -6.30	-1.75 -1.25 -2.52	0.32 0.40 1.06

(1) Kozeny-Carmen equation: $$K = \left(\frac{\rho g}{\mu}\right)\left[\frac{n^3}{(1-n^2)}\right]\left(\frac{d^2}{180}\right)$$

(2) Hazen equation: $K(m/day) = A(d_{10})^2$, A=1.0, d_{10} = grain diameter (mm)

(3) Krumbein-Monk equation: $K = 760(GM_d)^2(\theta^{-1.31\sigma})$, GM_d = Geometric mean diameter (mm), σ = standard deviation

(4) P = Permeability in cm^2; H = Hydraulic Conductivity in cm/sec.